

ACCELERATING ALTERNATING LEAST SQUARES FOR TENSOR DECOMPOSITION BY PAIRWISE PERTURBATION*

LINJIAN MA[†] AND EDGAR SOLOMONIK[‡]

Abstract. The alternating least squares algorithm for CP and Tucker decomposition is dominated in cost by the tensor contractions necessary to set up the quadratic optimization subproblems. We introduce a novel family of algorithms that uses perturbative corrections to the subproblems rather than recomputing the tensor contractions. This approximation is accurate when the factor matrices are changing little across iterations, which occurs when alternating least squares approaches convergence. We provide a theoretical analysis to bound the approximation error, leveraging a novel notion of the tensor condition number. Our numerical experiments demonstrate that the proposed pairwise perturbation algorithms are easy to control and converge to minima that are as good as alternating least squares. The performance of the new algorithms shows improvements of 1.3-2.8X with respect to state of the art alternating least squares approaches for various model tensor problems and real datasets on 1, 16 and 256 Intel KNL nodes of the Stampede2 supercomputer.

Key words. tensor, CP decomposition, Tucker decomposition, alternating least squares, tensor condition number

AMS subject classifications. 15A69, 15A72, 65F35, 65K10, 65Y20, 65Y04, 65Y05, 68W25

1. Introduction. Tensor decompositions provide general techniques for approximation and modeling of high dimensional data [11, 14, 18, 20, 30, 40]. They are fundamental in methods for computational chemistry [8, 24, 26], physics [37], and quantum information [25, 37]. Tensor decompositions are performed on tensors arising both in the context of numerical-PDEs (e.g. as part of preconditioners [39]) as well as in data-driven statistical modeling [2, 30, 33, 34]. The alternating least squares (ALS) method, which is most commonly used to compute many of these tensor decompositions, has become a target for parallelization [22, 27], performance optimization [12, 43], and acceleration by randomization [7]. We propose a new algorithm that asymptotically accelerates ALS iteration complexity for CP and Tucker decomposition by leveraging an approximation that is provably accurate for well-conditioned problems and is increasingly so as the algorithm approaches the optimization local minima.

Generally, ALS solves quadratic optimization subproblems for individual factors composing the decomposition. It does so in an alternating manner, updating every factor at each sweep. For both CP and Tucker decomposition, computational cost of each sweep is dominated by the tensor contractions needed to setup the quadratic optimization subproblem for every factor matrix. These contractions are redone at every ALS sweep since they involve the factor matrices, all of which change after each sweep. We propose to circumvent these contractions in the scenario when the factor matrices are changing only slightly at each sweep, which is expected when ALS approaches a local minima. Our method approximates the setup of each quadratic optimization subproblem by computing perturbative corrections due to the change in each factor matrices to the quadratic subproblems used for updating each other factor

*Submitted to the editors 11/26/2018.

Funding: The authors acknowledge the Texas Advanced Computing Center (TACC) at The University of Texas at Austin for providing HPC resources that have contributed to the research results reported within this paper. Project allocation: TG-CCR180006.

[†]Department of Electrical Engineering and Computer Sciences, University of California at Berkeley, Berkeley, CA, 94709 (linjian@berkeley.edu).

[‡]Department of Computer Science, University of Illinois at Urbana-Champaign, Urbana, IL, 61801 (solomon2@illinois.edu).

matrix. To do so, pairwise perturbative operators are computed that propagate the change to each factor matrix to the subproblem needed to update each other factor matrix. Computing these operators costs slightly more than a typical ALS iteration. These operators are then reused to *approximately* perform more ALS sweeps until the changes to the factor matrices are deemed large, at which point, the pairwise operators are recomputed. Each sweep computed approximately in this way costs asymptotically less than a regular ALS sweep.

For CP decomposition, CP-ALS [11,21] is widely used as it provides high-accuracy for the amount of computation required [30] (although alternatives based on gradient and subgradient descent are also competitive [1]). Within CP-ALS, the computational bottleneck of each iteration involves an operation called *the matricized tensor-times Khatri-Rao product* (MTTKRP). Similarly, the costliest operation in the ALS-based Tucker decomposition (Tucker-ALS) method is called *the tensor times matrix-chain* (TTMc) product. For an order N tensor with modes of dimension s , perturbative approximated computation of ALS sweeps reduces the cost of that sweep from $O(s^n R)$ to $O(s^2 R)$ for a rank- R CP decomposition and from $O(s^n R)$ to $O(s^2 R^{N-1})$ for a rank- R Tucker decomposition.

In order to bound the error incurred by the perturbative approximation, we define a tensor condition number in Section 3, which, for a tensor contracted with vectors along all except one mode, bounds the maximum relative output amplification vector due to any input perturbation to the input vectors. Both the MTTKRP and TTMc products in CP and rank- s Tucker decomposition, respectively, consist of a set of such contractions. We demonstrate that this condition number is the reciprocal of the distance to the nearest tensor which has a Tucker decomposition that results in a core tensor with a zero fiber. This tensor condition number generalizes the condition number of square matrices to equidimensional tensors, and provides a sensible extension to non-square matrices and non-equidimensional tensors.

To quantify the accuracy of the pairwise perturbation approximated algorithm, in Section 5, we provide an error analysis for both the MTTKRP and TTMc operations. For both operations, we bound the relative output error based on the relative magnitude of the perturbation to the factor matrices since the computation of the pairwise operators. We establish error bounds for both cases using the condition number of the input tensor. To achieve the same accuracy for the operation output, tighter restrictions are needed for MTTKRP operation compared to TTMc. For MTTKRP, the column-wise relative error of the output is $O(\epsilon^2 \kappa(\mathcal{X}))$ when the column-wise 2-norm relative perturbation of all input matrices are bounded by $O(\epsilon)$. For TTMc, we establish the same relationship as well as a similar bound, relating the matrix 2-norms of the output error and input perturbation. In addition, for the TTMc operation, we derive a condition-number-independent 2-norm relative error bound of $O(\epsilon^2)$ that holds when the residual of the Tucker decomposition is somewhat less than the norm of the original tensor. Finally, we derive a Frobenius norm error bound of $O(\epsilon^2 (s/R)^{N/2})$ for TTMc, which assumes only that HOSVD [15,46] is performed to initialize Tucker-ALS (which is typical).

In order to evaluate the performance benefit of pairwise perturbation, in Section 6, we compare kernels and full decomposition performance on one and many nodes of a Intel KNL system (Stampede2) of implementations developed using the Cyclops [44] and ScaLAPACK [9] libraries. Our microbenchmark results compare the strong and weak scaling performance of one ALS sweep of the dimension tree algorithm and the first/restart step, in which the pairwise perturbation operators are calculated, as well as the middle steps, in which the operators are not recalculated, of the pairwise

perturbation algorithm. These results show that the middle pairwise perturbation steps are 7.4-17.7X faster than one ALS sweep of the dimension tree algorithm in the weak scaling regime, while computing the pairwise operators takes no more than 2.6X the time of a dimension tree ALS sweep. We then study the performance and numerical behavior of pairwise perturbation for decomposition of synthetic tensors and application datasets. Our experimental results show that pairwise perturbation achieves as low residuals as standard ALS, and achieves typical speed-ups of 1.3-2.8X with respect to state of the art dimension tree based ALS algorithms on 1, 16, and 256 KNL nodes. Our results also show that with the increase of the input tensor size, the performance improvements increase, confirming the asymptotic cost improvement and indicating the potential of pairwise perturbation in large-scale data analysis.

2. Background. This section first outlines the notation that is used throughout this paper, then outlines the basic alternating least square algorithms for both CP and Tucker decomposition.

2.1. Notation and Definitions. Our analysis makes use of tensor algebra in both element-wise equations and specialized notation for tensor operations [30]. For vectors, bold lowercase Roman letters are used, e.g., \mathbf{x} . For matrices, bold uppercase Roman letters are used, e.g., \mathbf{X} . For tensors, bold calligraphic fonts are used, e.g., \mathcal{X} . An order N tensor corresponds to an N -dimensional array with dimensions $s_1 \times \dots \times s_N$. Elements of vectors, matrices, and tensors are denoted in parentheses, e.g., $\mathbf{x}(i)$ for a vector \mathbf{x} , $\mathbf{X}(i, j)$ for a matrix \mathbf{X} , and $\mathcal{X}(i, j, k, l)$ for an order 4 tensor \mathcal{X} . Columns of a matrix \mathbf{X} are denoted by $\mathbf{x}_i = \mathbf{X}(:, i)$.

The mode- n matrix product of a tensor $\mathcal{X} \in \mathbb{R}^{\prod_{i=1}^N s_i}$ with a matrix $\mathbf{A} \in \mathbb{R}^{J \times s_n}$ is denoted by $\mathcal{X} \times_n \mathbf{A}$, with the result having dimensions $s_1 \times \dots \times s_{n-1} \times J \times s_{n+1} \times \dots \times s_N$. By juxtaposition of tensor \mathcal{X} and a matrix \mathbf{M} , we denote the mode- N product with the transpose of the matrix, $\mathcal{X}\mathbf{M} = \mathcal{X} \times_N \mathbf{M}^T$. Matricization is the process of unfolding a tensor into a matrix. Given a tensor \mathcal{X} the mode- n matricized version is denoted by $\mathbf{X}_{(n)} \in \mathbb{R}^{s_n \times K}$ where $K = \prod_{m=1, m \neq n}^N s_m$. We generalize this notation to define the unfoldings of a tensor \mathcal{X} with dimensions $\prod_{m=1}^N s_m$ into an order $M + 1$ tensor, $\mathcal{X}_{(i_1, \dots, i_M)} \in \mathbb{R}^{s_{i_1} \times \dots \times s_{i_M} \times K}$, where $K = \prod_{i \in \{1, \dots, N\} \setminus \{i_1, \dots, i_M\}} s_i$, e.g.,

$$\mathcal{X}(j, k, l, m) = \mathcal{X}_{(1,3)}(j, l, k + (m - 1) \cdot s_2).$$

We use parenthesized superscripts as labels for different tensors, e.g., $\mathcal{X}^{(1)}$ and $\mathcal{X}^{(2)}$ are generally unrelated tensors.

The Hadamard product of two matrices $\mathbf{U}, \mathbf{V} \in \mathbb{R}^{I \times J}$ resulting in matrix $\mathbf{W} \in \mathbb{R}^{I \times J}$ is denoted by $\mathbf{W} = \mathbf{U} * \mathbf{V}$, where $\mathbf{W}(i, j) = \mathbf{U}(i, j)\mathbf{V}(i, j)$. The outer product of K vectors $\mathbf{u}^{(1)}, \dots, \mathbf{u}^{(K)}$ of corresponding sizes s_1, \dots, s_K is denoted by $\mathcal{X} = \mathbf{u}^{(1)} \circ \dots \circ \mathbf{u}^{(K)}$ where $\mathcal{X} \in \mathbb{R}^{\prod_{m=1}^K s_m}$ is an order K tensor. The Kronecker product of vectors $\mathbf{u} \in \mathbb{R}^I$ and $\mathbf{v} \in \mathbb{R}^J$ is denoted by $\mathbf{w} = \mathbf{u} \otimes \mathbf{v}$ where $\mathbf{w} \in \mathbb{R}^{IJ}$. For matrices $\mathbf{A} \in \mathbb{R}^{I \times K} = [\mathbf{a}^{(1)} \ \dots \ \mathbf{a}^{(K)}]$ and $\mathbf{B} \in \mathbb{R}^{J \times K} = [\mathbf{b}^{(1)} \ \dots \ \mathbf{b}^{(K)}]$, their Khatri-Rao product resulting in a matrix of size $(IJ) \times K$ defined by

$$\mathbf{A} \odot \mathbf{B} = [\mathbf{a}^{(1)} \otimes \mathbf{b}^{(1)}, \dots, \mathbf{a}^{(K)} \otimes \mathbf{b}^{(K)}].$$

2.2. CP Decomposition with ALS. The CP tensor decomposition [21, 23] is a higher-order generalization of the matrix singular value decomposition (SVD). The CP decomposition is denoted by

$$\mathcal{X} \approx \llbracket \mathbf{A}^{(1)}, \dots, \mathbf{A}^{(N)} \rrbracket, \quad \text{where} \quad \mathbf{A}^{(i)} = [\mathbf{a}_1^{(i)}, \dots, \mathbf{a}_r^{(i)}],$$

and serves to approximate a tensor by a sum of R tensor products of vectors:

$$\boldsymbol{\mathcal{X}} \approx \sum_{r=1}^R \mathbf{a}_r^{(1)} \circ \dots \circ \mathbf{a}_r^{(N)}.$$

The CP-ALS method alternates among quadratic optimization problems for each of the factor matrices $\mathbf{A}^{(n)}$, resulting in linear least squares problems for each row,

$$\mathbf{A}^{(n)} \mathbf{P}^{(n)T} \cong \mathbf{X}_{(n)},$$

where the matrix $\mathbf{P}^{(n)} \in \mathbb{R}^{I_n \times R}$, where $I_n = s_1 \times \dots \times s_{n-1} \times s_{n+1} \times \dots \times s_N$ is formed by Khatri-Rao products of the other factor matrices,

$$\mathbf{P}^{(n)} = \mathbf{A}^{(1)} \odot \dots \odot \mathbf{A}^{(n-1)} \odot \mathbf{A}^{(n+1)} \odot \dots \odot \mathbf{A}^{(N)}.$$

These linear least squares problems are often solved via the normal equations [30]. We also adopt this strategy here to devise the pairwise perturbation method. The normal equations for the n th factor matrix are

$$\mathbf{A}^{(n)} \boldsymbol{\Gamma}^{(n)} \leftarrow \mathbf{X}_{(n)} \mathbf{P}^{(n)},$$

where $\boldsymbol{\Gamma} \in \mathbb{R}^{r \times r}$ can be computed via

$$\begin{aligned} \boldsymbol{\Gamma}^{(n)} &= \mathbf{S}^{(1)} * \dots * \mathbf{S}^{(n-1)} * \mathbf{S}^{(n+1)} * \dots * \mathbf{S}^{(N)}, \\ &\text{with each } \mathbf{S}^{(i)} = \mathbf{A}^{(i)T} \mathbf{A}^{(i)}. \end{aligned}$$

These equations also give the n th component of the optimality conditions for the unconstrained minimization of the nonlinear objective function,

$$f(\mathbf{A}^{(1)}, \dots, \mathbf{A}^{(N)}) = \frac{1}{2} \|\boldsymbol{\mathcal{X}} - \llbracket \mathbf{A}^{(1)}, \dots, \mathbf{A}^{(N)} \rrbracket\|_F^2,$$

for which the n th component of the gradient is

$$\frac{\partial f}{\partial \mathbf{A}^{(n)}} = \mathbf{G}^{(n)} = \mathbf{A}^{(n)} \boldsymbol{\Gamma}^{(n)} - \mathbf{X}_{(n)} \mathbf{P}^{(n)} = (\mathbf{A}^{(n)} - \mathbf{A}_{\text{new}}^{(n)}) \boldsymbol{\Gamma}^{(n)}.$$

Algorithm 2.1 presents the basic ALS method described above, keeping track of the Frobenius norm of the N components of the overall gradient to ascertain convergence.

The *Matricized Tensor Times Khatri-Rao Product* or MTTKRP computation $\mathbf{M}^{(n)} = \mathbf{X}_{(n)} \mathbf{P}^{(n)}$ is the main computational bottleneck of CP-ALS [6]. The computational cost of MTTKRP is $\Theta(s^N R)$ if $s_n = s$ for all $n \in \{1, \dots, N\}$. The tensor contractions necessary for MTTKRP can be amortized across the linear least squares problems necessary for a given ALS sweep (while loop iteration in Algorithm 2.1). With the best choice of dimension trees [6, 29, 41, 48] to calculate $\mathbf{M}^{(n)}$ in one ALS iteration, to leading order in s , the computational complexity is $4s^N R$. The normal equations worsen the conditioning, but are advantageous for CP-ALS, since $\boldsymbol{\Gamma}^{(n)}$ can be computed and inverted in just $O(s^2 R + R^3)$ cost and the MTTKRP can be amortized by dimension trees. If QR is used instead of the normal equations, the product of \mathbf{Q} with the right-hand sides would have the cost $2s^N R$ and would need to be done for each linear least squares problem, increasing the overall leading order cost by a factor of $N/2$. Our pairwise perturbation algorithm amortizes the dominant cost of the computation of $\mathbf{M}^{(n)} = \mathbf{X}_{(n)} \mathbf{P}^{(n)}$ across multiple ALS sweeps.

Algorithm 2.1 CP_ALS: ALS procedure for CP decomposition

```

1: Input: Tensor  $\mathcal{X} \in \mathbb{R}^{\prod_{i=1}^N s_i}$ , stopping criteria  $\varepsilon$ 
2: Initialize  $\llbracket \mathbf{A}^{(1)}, \dots, \mathbf{A}^{(N)} \rrbracket$ 
3: while  $\sum_{i=1}^N \|\mathbf{G}^{(i)}\|_F > \varepsilon$  do
4:   for  $n \in \{1, \dots, N\}$  do
5:      $\mathbf{\Gamma}^{(n)} \leftarrow \mathbf{S}^{(1)} * \dots * \mathbf{S}^{(n-1)} * \mathbf{S}^{(n+1)} * \dots * \mathbf{S}^{(N)}$ 
6:      $\mathbf{M}^{(n)} \leftarrow \mathbf{X}_{(n)}(\mathbf{A}^{(1)} \odot \dots \odot \mathbf{A}^{(n-1)} \odot \mathbf{A}^{(n+1)} \odot \dots \odot \mathbf{A}^{(N)})$ 
7:      $\mathbf{A}_{\text{new}}^{(n)} \leftarrow \mathbf{M}^{(n)} \mathbf{\Gamma}^{(n)\dagger}$ 
8:      $\mathbf{G}^{(n)} \leftarrow (\mathbf{A}^{(n)} - \mathbf{A}_{\text{new}}^{(n)}) \mathbf{\Gamma}^{(n)}$ 
9:      $\mathbf{A}^{(n)} \leftarrow \mathbf{A}_{\text{new}}^{(n)}$ 
10:     $\mathbf{S}^{(n)} \leftarrow \mathbf{A}^{(n)T} \mathbf{A}^{(n)}$ 
11:   end for
12: end while
13: return  $\llbracket \mathbf{A}^{(1)}, \dots, \mathbf{A}^{(N)} \rrbracket$ 

```

Algorithm 2.2 Tucker_ALS: ALS procedure for Tucker decomposition

```

1: Input: Tensor  $\mathcal{X} \in \mathbb{R}^{\prod_{i=1}^N s_i}$ , decomposition ranks  $\{R_1, \dots, R_N\}$ , stopping criteria  $\varepsilon$ 
2: Initialize  $\llbracket \mathcal{G}; \mathbf{A}^{(1)}, \dots, \mathbf{A}^{(N)} \rrbracket$  using HOSVD
3: while  $\|\mathcal{F}\|_F > \varepsilon$  do
4:   for  $n \in \{1, \dots, N\}$  do
5:      $\mathcal{Y} \leftarrow \mathcal{X} \times_1 \mathbf{A}^{(1)T} \dots \times_{n-1} \mathbf{A}^{(n-1)T} \times_{n+1} \mathbf{A}^{(n+1)T} \dots \times_N \mathbf{A}^{(N)T}$ 
6:      $\mathbf{A}^{(n)} \leftarrow R_n$  leading left singular vectors of  $\mathbf{Y}_{(n)}$ 
7:   end for
8:    $\mathcal{G}_{\text{new}} \leftarrow \mathcal{X} \times_1 \mathbf{A}^{(1)T} \dots \times_N \mathbf{A}^{(N)T}$ 
9:    $\mathcal{F} \leftarrow \mathcal{G}_{\text{new}} - \mathcal{G}$ 
10:   $\mathcal{G} \leftarrow \mathcal{G}_{\text{new}}$ 
11: end while
12: return  $\llbracket \mathcal{G}; \mathbf{A}^{(1)}, \dots, \mathbf{A}^{(N)} \rrbracket$ 

```

2.3. Tucker Decomposition with ALS. In this section we review the ALS method for computing a low-rank Tucker decomposition of a tensor [46]. Tucker decomposition approximates a tensor by a core tensor contracted by orthogonal matrices along each mode. The Tucker decomposition is given by

$$\mathcal{X} \approx \llbracket \mathcal{G}; \mathbf{A}^{(1)}, \dots, \mathbf{A}^{(N)} \rrbracket = \mathcal{G} \times_1 \mathbf{A}^{(1)} \times_2 \mathbf{A}^{(2)} \dots \times_N \mathbf{A}^{(N)}.$$

The corresponding element-wise expression is

$$\mathcal{X}(x_1, \dots, x_N) \approx \sum_{\{z_1, \dots, z_N\}} \mathcal{G}(z_1, \dots, z_N) \prod_{r \in \{1, \dots, N\}} \mathbf{A}^{(r)}(x_r, z_r).$$

The core tensor \mathcal{G} is of order N with dimensions (Tucker ranks) $R_1 \times \dots \times R_N$ (throughout error and cost analysis we assume each $R_n = R$ for $n \in \{1, \dots, N\}$). The matrices $\mathbf{A}^{(n)} \in \mathbb{R}^{s_n \times R_n}$ have orthonormal columns.

The *higher-order singular value decomposition* (HOSVD) [15, 46] computes the leading left singular vectors of each one-mode unfolding of \mathcal{X} , providing a good starting point for the Tucker-ALS algorithm. The classical HOSVD computes the truncated SVD of $\mathbf{X}_{(n)} \approx \mathbf{U}^{(n)} \mathbf{\Sigma}^{(n)} \mathbf{V}^{(n)T}$ and sets $\mathbf{A}^{(n)} = \mathbf{U}^{(n)}$ for $n \in \{1, \dots, N\}$. The interlaced HOSVD [19, 49] instead computes the truncated SVD of

$$\mathbf{Z}_{(n)}^{(n)} = \mathbf{U}^{(n)} \mathbf{\Sigma}^{(n)} \mathbf{V}^{(n)T} \quad \text{where} \quad \mathbf{Z}^{(1)} = \mathcal{X} \quad \text{and} \quad \mathbf{Z}_{(n)}^{(n+1)} = \mathbf{\Sigma}^{(n)} \mathbf{V}^{(n)T}.$$

The interlaced HOSVD is cheaper, since the size of each $\mathbf{Z}^{(n)}$ is $s^{N-n+1}R^{n-1}$.

The ALS method for Tucker decomposition [3, 16, 30], which is also called the *higher-order orthogonal iteration* (HOOI), then proceeds by fixing all except one factor matrix, and computing a low-rank matrix factorization to update that factor matrix and the core tensor. To update the n th factor matrix Tucker-ALS factorizes

$$\mathbf{Y}^{(n)} = \mathbf{X} \times_1 \mathbf{A}^{(1)T} \dots \times_{n-1} \mathbf{A}^{(n-1)T} \times_{n+1} \mathbf{A}^{(n+1)T} \dots \times_N \mathbf{A}^{(N)T}$$

into a product of an orthogonal matrix $\mathbf{A}^{(n)}$ and the core tensor \mathcal{G} , so that $\mathbf{Y}_{(n)}^{(n)} \approx \mathbf{A}^{(n)} \mathbf{G}_{(n)}$. This factorization can be done by taking $\mathbf{A}^{(n)}$ to be the R_n leading left singular vectors of $\mathbf{Y}_{(n)}^{(n)}$. This Tucker-ALS procedure is given in Algorithm 2.2.

As in previous work [13, 38], our implementation computes these singular vectors by finding the left eigenvectors of the Gram matrix $\mathbf{W} = \mathbf{Y}_{(n)}^{(n)} \mathbf{Y}_{(n)}^{(n)T}$. Computing the Gram matrix sacrifices some numerical stability, but avoids a large SVD and provides consistency of the signs of the singular vectors across ALS sweeps.

The *Tensor Times Matrix-chain* or TTMc computes each $\mathbf{Y}^{(n)}$ and is the main computational bottleneck of Tucker-ALS [28]. With the use of dimensions trees [6, 29, 41, 48] to calculate $\mathbf{Y}^{(n)}$ in one ALS sweep, the computational complexity for each while loop iteration in Algorithm 2.2 to leading order in s is $4s^N R$.

3. Tensor Conditioning. Our error analysis makes use of bounds on the spectral norm and condition number of tensors. We introduce a notion of a tensor condition number that corresponds to a global bound on the conditioning of the multilinear vector-valued function, $\mathbf{g}_{\mathcal{T}} : \otimes_{i=1}^{N-1} \mathbb{R}^{s_{i+1}} \rightarrow \mathbb{R}^{s_1}$ associated with the product of the tensor with vectors along all except the first mode,

$$\mathbf{g}_{\mathcal{T}}(\mathbf{x}_1, \dots, \mathbf{x}_{N-1}) = \mathbf{T}_{(1)}(\mathbf{x}_1 \circ \dots \circ \mathbf{x}_{N-1}).$$

The norm and condition number are given by extrema of the norm amplification of $\mathbf{g}_{\mathcal{T}}$, which are described by the amplification function $\mathbf{f}_{\mathcal{T}} : \otimes_{i=1}^{N-1} \mathbb{R}^{s_{i+1}} \rightarrow \mathbb{R}$,

$$\mathbf{f}_{\mathcal{T}}(\mathbf{x}_1, \dots, \mathbf{x}_{N-1}) = \frac{\|\mathbf{g}_{\mathcal{T}}(\mathbf{x}_1, \dots, \mathbf{x}_{N-1})\|_2}{\|\mathbf{x}_1\|_2 \dots \|\mathbf{x}_{N-1}\|_2}.$$

The spectral norm of the tensor corresponds to its supremum,

$$\|\mathcal{T}\|_2 = \sup\{\mathbf{f}_{\mathcal{T}}\}.$$

The tensor condition number is then defined as

$$\kappa(\mathcal{T}) = \sup\{\mathbf{f}_{\mathcal{T}}\} / \inf\{\mathbf{f}_{\mathcal{T}}\},$$

which enables quantification of the worst-case relative amplification of error with respect to input for the product of a tensor with vectors along all except one mode. In particular, $\kappa(\mathcal{T})$ provides an upper bound on the relative norm of the perturbation of $\mathbf{g}_{\mathcal{T}}$ with respect to the relative norm of any perturbation to any input vector. This tensor condition number should not be confused with the conditioning of CP decomposition [10, 17, 47].

3.1. Tensor Norm. The spectral norm of any tensor $\mathcal{T} \in \mathbb{R}^{\otimes_{i=1}^N s_i}$ is

$$\|\mathcal{T}\|_2 = \max_{\substack{\forall i \in \{1, \dots, N-1\}, \mathbf{x}_i \in \mathbb{R}^{s_{i+1}} \\ \|\mathbf{x}_1\|_2 = \dots = \|\mathbf{x}_{N-1}\|_2 = 1}} \|\mathbf{T}_{(1)}(\mathbf{x}_1 \circ \dots \circ \mathbf{x}_{N-1})\|_2.$$

The spectral tensor norm corresponds to the magnitude of the largest tensor singular value [32] and is invariant under reordering of modes of \mathcal{T} . Lemma 3.1 shows submultiplicativity of this norm for the tensor times matrix product.

LEMMA 3.1. *Given any tensor $\mathcal{T} \in \mathbb{R}^{\otimes_{i=1}^N s_i}$ and matrix $\mathbf{M} \in \mathbb{R}^{s_N \times R}$, if $\mathcal{V} = \mathcal{T}\mathbf{M}$ then $\|\mathcal{V}\|_2 \leq \|\mathcal{T}\|_2 \|\mathbf{M}\|_2$.*

Proof. Assume $\|\mathcal{V}\|_2 > \|\mathcal{T}\|_2 \|\mathbf{M}\|_2$, then there exist unit vectors $\mathbf{x}_1, \dots, \mathbf{x}_{N-1}$ such that

$$\|\mathcal{V}\|_2 = \|\mathbf{V}_{(N)}(\mathbf{x}_1 \circ \dots \circ \mathbf{x}_{N-1})\|_2 = \|\mathbf{T}_{(N)}(\mathbf{x}_1 \circ \dots \circ \mathbf{x}_{N-2} \circ \mathbf{M}\mathbf{x}_{N-1})\|_2.$$

Let $\mathbf{z} = \mathbf{M}\mathbf{x}_{N-1}$, so $\|\mathbf{z}\|_2 \leq \|\mathbf{M}\|_2$. We arrive at a contradiction, since

$$\|\mathbf{T}_{(N)}(\mathbf{x}_1 \circ \dots \circ \mathbf{x}_{N-2} \circ \mathbf{z})\|_2 \leq \|\mathbf{T}_{(N)}(\mathbf{x}_1 \circ \dots \circ \mathbf{x}_{N-2} \circ \mathbf{z})\|_2 \frac{\|\mathbf{M}\|_2}{\|\mathbf{z}\|_2} \leq \|\mathcal{T}\|_2 \|\mathbf{M}\|_2. \square$$

3.2. Tensor Condition Number. We define the condition number of a tensor as the ratio of the supremum and infimum of the aforementioned function $\mathbf{f}_{\mathcal{T}}$. For a matrix $\mathbf{M} \in \mathbb{R}^{s_1 \times s_2}$, if $s_1 > s_2$ this corresponds to defining $\kappa(\mathbf{M}) = \sigma_{\max}(\mathbf{M})/\sigma_{\min}(\mathbf{M})$ where $\sigma_{\min}(\mathbf{M})$ is the smallest singular value of \mathbf{M} in the reduced SVD, while if $s_1 < s_2$, then $\kappa(\mathbf{M}) = \infty$. Generally, for any tensor $\mathcal{T} \in \mathbb{R}^{\otimes_{i=1}^N s_i}$ the condition number is

$$\kappa(\mathcal{T}) = \|\mathcal{T}\|_2 / \min_{\substack{\forall i \in \{1, \dots, N-1\}, \mathbf{x}_i \in \mathbb{R}^{s_i+1} \\ \|\mathbf{x}_1\|_2 = \dots = \|\mathbf{x}_{N-1}\|_2 = 1}} \|\mathbf{T}_1(\mathbf{x}_1 \circ \dots \circ \mathbf{x}_{N-1})\|_2.$$

When tensor dimensions are unequal, the condition number is infinite if the first dimension is not the largest, so for some i , $s_i > s_1$. Aside from this condition, the ordering of modes of \mathcal{T} does not affect the condition number, since for any $m > 1$, the supremum/infimum of $\mathbf{f}_{\mathcal{T}}$ over the domain of unit vectors are for some choice of $\mathbf{x}^{(1)}, \dots, \mathbf{x}^{(m-1)}, \mathbf{x}^{(m+1)}, \dots, \mathbf{x}^{(N-1)}$ the maximum/minimum singular values of

$$\mathbf{K} = \mathcal{T}_{(1,m)}(\mathbf{x}^{(1)} \circ \dots \circ \mathbf{x}^{(m-1)} \circ \mathbf{x}^{(m+1)} \circ \dots \circ \mathbf{x}^{(N-1)}).$$

To demonstrate that this condition number can be bounded for tensors of order greater than 2, we provide two examples of order three tensors that have unit condition number. The first example has $s_i = 2$, and yields a Givens rotation when contracted with a vector along the last mode. It is composed of two slices:

$$\begin{bmatrix} 1 & \\ & 1 \end{bmatrix} \quad \text{and} \quad \begin{bmatrix} & 1 \\ -1 & \end{bmatrix}.$$

The second example has $s_i = 4$ and is composed of four slices:

$$\begin{bmatrix} 1 & & & \\ & 1 & & \\ & & 1 & \\ & & & -1 \end{bmatrix}, \begin{bmatrix} & 1 & & \\ -1 & & & \\ & & 1 & \\ & & & 1 \end{bmatrix}, \begin{bmatrix} & & 1 & \\ & & & 1 \\ 1 & & & \\ & -1 & & \end{bmatrix}, \begin{bmatrix} & & & -1 \\ & & & 1 \\ 1 & & & \\ & 1 & & \end{bmatrix}.$$

The fact that this tensor has unit condition number can be verified by symbolic algebraic manipulation or numerical tests. Other perfectly conditioned tensors can be obtained by multiplying the above tensors by an orthogonal matrix along any mode

(we prove below that such transformations preserve condition number), but currently we do not know how to construct tensors of other order/dimensions with bounded condition number.

In our analysis, we make use of the following submultiplicativity property of the tensor condition number with respect to tensor times matrix products (the property also generalizes to pairs of arbitrary order tensors contracted over one mode).

LEMMA 3.1. *For any $\mathcal{T} \in \mathbb{R}^{\otimes_{i=1}^N s_i}$ and matrix \mathbf{M} , if $\mathcal{V} = \mathcal{T}\mathbf{M}$ then $\kappa(\mathcal{V}) \leq \kappa(\mathcal{T})\kappa(\mathbf{M})$.*

Proof. Assume $\kappa(\mathcal{V}) > \kappa(\mathcal{T})$, then there exist unit vectors $\mathbf{x}_1, \dots, \mathbf{x}_{N-1}$ and $\mathbf{y}_1, \dots, \mathbf{y}_{N-1}$ such that

$$\kappa(\mathcal{T}) < \kappa(\mathcal{V}) = \frac{\|\mathbf{V}_{(N)}(\mathbf{x}_1 \circ \dots \circ \mathbf{x}_{N-1})\|_2}{\|\mathbf{V}_{(N)}(\mathbf{y}_1 \circ \dots \circ \mathbf{y}_{N-1})\|_2} = \frac{\|\mathbf{T}_{(1)}(\mathbf{x}_1 \circ \dots \circ \mathbf{x}_{N-2} \circ \mathbf{M}\mathbf{x}_{N-1})\|_2}{\|\mathbf{T}_{(1)}(\mathbf{y}_1 \circ \dots \circ \mathbf{y}_{N-2} \circ \mathbf{M}\mathbf{y}_{N-1})\|_2}.$$

Let $\mathbf{u} = \mathbf{M}\mathbf{x}_{N-1}$ and $\mathbf{v} = \mathbf{M}\mathbf{y}_{N-1}$, so $\|\mathbf{u}\|_2/\|\mathbf{v}\|_2 \leq \kappa(\mathbf{M})$, yielding a contradiction,

$$\kappa(\mathcal{V}) \leq \frac{\|\mathbf{T}_{(1)}(\mathbf{x}_1 \circ \dots \circ \mathbf{x}_{N-2} \circ (\mathbf{u}/\|\mathbf{u}\|_2))\|_2}{\|\mathbf{T}_{(1)}(\mathbf{y}_1 \circ \dots \circ \mathbf{y}_{N-2} \circ (\mathbf{v}/\|\mathbf{v}\|_2))\|_2} \kappa(\mathbf{M}) \leq \kappa(\mathcal{T})\kappa(\mathbf{M}). \quad \square$$

Applying Lemma 3.1 with a vector, i.e. when $\mathbf{M} \in \mathbb{R}^{s_N \times 1}$ and so has condition number $\kappa(\mathbf{M}) = 1$, implies $\kappa(\mathcal{T}\mathbf{M}) \leq \kappa(\mathcal{T})$. By an analogous argument to the proof of Lemma 3.1, we can also conclude that the norm and infimum of such a product of \mathcal{T} with unit vectors are bounded by those of \mathcal{T} , giving the following corollary.

COROLLARY 3.2. *For any $\mathcal{T} \in \mathbb{R}^{\otimes_{i=1}^N s_i}$, vector $\mathbf{u} \in \mathbb{R}^{s_n}$, and any $n \in \{1, \dots, N\}$ such that $\exists m \in \{1, \dots, N\}$ with $s_m \geq s_n$ and $m \neq n$, if $\mathcal{V} = \mathcal{T} \times_n \mathbf{u}$, then $\|\mathcal{V}\|_2 \leq \|\mathbf{u}\|_2 \|\mathcal{T}\|_2$, $\inf\{\mathbf{f}_{\mathcal{V}}\} \geq \|\mathbf{u}\|_2 \inf\{\mathbf{f}_{\mathcal{T}}\}$, and $\kappa(\mathcal{V}) \leq \kappa(\mathcal{T})$.*

For an orthogonal matrix \mathbf{M} , Lemma 3.1 can be applied in both directions, namely for $\mathcal{V} = \mathcal{T}\mathbf{M}$ and $\mathcal{T} = \mathcal{V}\mathbf{M}^T$, so we observe that $\kappa(\mathcal{V}) = \kappa(\mathcal{T})$. Using this fact, we demonstrate in the following theorem that any tensor \mathcal{T} can be transformed by orthogonal matrices along each mode, so that one of its fibers has norm $\|\mathcal{T}\|_2/\kappa(\mathcal{T})$.

THEOREM 3.2. *For any $\mathcal{T} \in \mathbb{R}^{\otimes_{i=1}^N s_i}$, there exist orthogonal matrices $\mathbf{Q}_1 \dots \mathbf{Q}_{N-1}$, with $\mathbf{Q}_i \in \mathbb{R}^{s_{i+1} \times s_{i+1}}$, such that $\mathcal{V} = \mathcal{T} \times_2 \mathbf{Q}_1 \cdots \times_N \mathbf{Q}_{N-1}$ satisfies $\kappa(\mathcal{V}) = \kappa(\mathcal{T})$, $\|\mathcal{V}\|_2 = \|\mathcal{T}\|_2$, and the first fiber of \mathcal{V} , i.e. the vector \mathbf{v} with $\mathbf{v}(i) = \mathcal{V}(i, 0, \dots, 0)$, satisfies $\|\mathbf{v}\|_2 = \|\mathcal{T}\|_2/\kappa(\mathcal{T})$.*

Proof. Given a tensor \mathcal{T} with infinite condition number, there must exist $N-1$ unit vectors $\mathbf{x}_1, \dots, \mathbf{x}_n$, such that $\|\mathbf{T}_1(\mathbf{x}_1 \circ \dots \circ \mathbf{x}_{N-1})\|_2 = \|\mathcal{T}\|_2/\kappa(\mathcal{T})$. We define $N-1$ orthogonal matrices $\mathbf{Q}_1, \dots, \mathbf{Q}_{N-1}$ such that $\mathbf{Q}_i^T \mathbf{x}_i = \mathbf{e}_1$. We can then contract \mathcal{T} with these matrices along the last $N-1$ modes, resulting in \mathcal{V} , with the same condition number as \mathcal{T} (by Lemma 3.1) and the same norm (by a similar argument). Then, we have that the first fiber of \mathcal{V} is

$$\mathbf{v} = \mathbf{V}_1(\mathbf{e}_1 \circ \dots \circ \mathbf{e}_1) = \mathbf{T}_1(\mathbf{x}_1 \circ \dots \circ \mathbf{x}_{N-1}),$$

and consequently $\|\mathbf{v}\|_2 = \|\mathcal{T}\|_2/\kappa(\mathcal{T})$. \square

By Theorem 3.2, the condition number of a tensor is infinity if and only if it can be transformed by products with orthogonal matrices along the last $N-1$ modes into a tensor with a zero fiber. Further, any tensor \mathcal{T} may be perturbed to have infinite condition number by adding to it some $\delta\mathcal{T}$ with relative norm $\|\delta\mathcal{T}\|_2/\|\mathcal{T}\|_2 = 1/\kappa(\mathcal{T})$.

4. Pairwise Perturbation Algorithms. We now introduce a pairwise perturbation (PP) algorithm to accelerate the ALS procedure when the iterative optimization steps are approaching a local minimum. We first focus on deriving the approximation that asymptotically reduces the cost complexity, then in Section 4.3, provide algorithms that minimize constant factors in cost via dimension trees [6, 29, 41, 48]. The key idea of the pairwise perturbation method is to compute *pairwise perturbation operators*, which correlate a pair of factor matrices. These tensors are then used to repeatedly update the quadratic subproblems for each tensor. As we will show, these updates are provably accurate if the factor matrices do not change significantly since their state at the time of formation of the pairwise perturbation operators.

TABLE 1

Cost comparison between pairwise perturbation algorithm and state of the art (dimension tree) ALS algorithm for CP and Tucker decompositions.

	State of the art ALS	PP operator construction	PP middle steps
CP	$4s^N R$	$6s^N R$	$2Ns^2 R$
Tucker	$4s^N R$	$6s^N R$	$2Ns^2 R^{N-1}$

4.1. CP-ALS. The pairwise perturbation procedure for CP decomposition approximates $\mathbf{M}^{(n)} \approx \tilde{\mathbf{M}}^{(n)}$ (defined in Section 2.2) using pairwise perturbation operators $\mathcal{M}^{(i,n)}$ for $i \in \{1, \dots, n-1, n+1, \dots, N\}$. Below, we define these and more general partially contracted MTTKRP intermediates.

DEFINITION 4.1. $\mathcal{M}^{(i_1, i_2, \dots, i_m)}$ is defined as follows,

$$\mathcal{M}^{(i_1, i_2, \dots, i_m)} = \mathcal{X}_{(i_1, i_2, \dots, i_m)} \bigcirc_{j \in \{1, \dots, N\} \setminus \{i_1, i_2, \dots, i_m\}} \mathbf{A}^{(j)}.$$

Element-wise, we have $\mathcal{M}^{(i_1, i_2, \dots, i_m)}(x_{i_1}, x_{i_2}, \dots, x_{i_m}, k) =$

$$\sum_{\{x_1, \dots, x_N\} \setminus \{x_{i_1}, x_{i_2}, \dots, x_{i_m}\}} \mathcal{X}(x_1, \dots, x_N) \prod_{r \in \{1, \dots, N\} \setminus \{i_1, i_2, \dots, i_m\}} \mathbf{A}^{(r)}(x_r, k).$$

Let $\mathbf{A}_p^{(n)}$ denote the $\mathbf{A}^{(n)}$ calculated with a regular ALS step, some number of steps prior to the current one. Then $\mathbf{A}^{(n)}$ at the current step can be expressed as

$$\mathbf{A}^{(n)} = \mathbf{A}_p^{(n)} + d\mathbf{A}^{(n)},$$

and $\mathbf{M}^{(n)}$ can be expressed as

$$\mathbf{M}^{(n)} = \mathbf{X}_{(n)} \bigcirc_{i=1, i \neq n}^N (\mathbf{A}_p^{(i)} + d\mathbf{A}^{(i)}).$$

The expression above can be rewritten as a function of $\mathcal{M}_p^{(i_1, i_2, \dots, i_m)}$, which is defined in the same way as $\mathcal{M}^{(i_1, i_2, \dots, i_m)}$ except that \mathcal{X} is contracted with $\mathbf{A}_p^{(j)}$ for $j \in \{1, \dots, N\} \setminus \{i_1, i_2, \dots, i_m\}$. $\mathbf{M}^{(n)}$ can be expressed as follows,

$$\begin{aligned} \mathbf{M}^{(n)}(y, k) = & \mathbf{M}_p^{(n)}(y, k) + \sum_{i=1, i \neq n}^N \sum_{x=1}^{s_i} \mathcal{M}_p^{(i,n)}(x, y, k) d\mathbf{A}^{(i)}(x, k) + \\ & \sum_{i=1, i \neq n}^N \sum_{j=i+1, j \neq n}^N \sum_{x=1}^{s_i} \sum_{z=1}^{s_j} \mathcal{M}_p^{(i,j,n)}(x, z, y, k) d\mathbf{A}^{(i)}(x, k) d\mathbf{A}^{(j)}(z, k) + \dots \end{aligned}$$

From the above expression we observe that except the first two terms, all terms include the contraction between tensor $\mathcal{M}_p^{(i_1, i_2, \dots, i_m)}$ and at least two matrices $d\mathbf{A}^{(i)}$, which are small in norm when each $d\mathbf{A}^{(i)}$ is small in norm. The pairwise perturbation algorithm obtains an effective approximation by computing only the first two terms (these terms are described by Figure 1):

$$\tilde{\mathbf{M}}^{(n)}(y, k) = \mathbf{M}_p^{(n)}(y, k) + \sum_{i=1, i \neq n}^N \sum_{x=1}^{s_i} \mathcal{M}_p^{(i, n)}(x, y, k) d\mathbf{A}^{(i)}(x, k),$$

$$\text{where } \mathbf{M}_p^{(n)} = \mathbf{X}_{(n)} \bigcirc_{i=1, i \neq n}^N \mathbf{A}_p^{(i)}, \quad \text{and } \mathcal{M}_p^{(i, n)} = \mathcal{X}_{(i, n)} \bigcirc_{j \in \{1, \dots, N\} \setminus \{i, n\}}^N \mathbf{A}_p^{(j)}.$$

Given $\mathcal{M}_p^{(i, n)}$ and $\mathbf{M}_p^{(n)}$, calculation of $\tilde{\mathbf{M}}^{(n)}$ for $n \in \{1, \dots, N\}$ requires $2Ns^2R$ operations overall. Further, we show in Section 5.1 that the column-wise relative approximation error of $\tilde{\mathbf{M}}^{(n)}$ with respect to $\mathbf{M}^{(n)}$ is small if each $\frac{\|d\mathbf{a}_k^{(n)}\|_2}{\|\mathbf{a}_k^{(n)}\|_2}$ for $n \in \{1, \dots, N\}, k \in \{1, \dots, R\}$ is sufficiently small. Algorithm 4.1 presents the PP-CP-ALS method described above.

Algorithm 4.1 CP-ALS-PP: Pairwise perturbation procedure for CP-ALS

- 1: **Input:** tensor $\mathcal{X} \in \mathbb{R}^{\prod_{i=1}^N s_i}$, stopping criteria ε , PP tolerance ϵ
 - 2: Initialize $[\mathbf{A}^{(1)}, \dots, \mathbf{A}^{(N)}]$
 - 3: **while** $\sum_{i=1}^N \|\mathbf{G}^{(i)}\|_F > \varepsilon$ **do**
 - 4: **if** $\forall i \in \{1, \dots, N\}, \|d\mathbf{A}^{(i)}\|_F < \epsilon$ **then**
 - 5: Compute $\mathcal{M}_p^{(i, n)}, \mathbf{M}_p^{(n)}$ for $i, n \in \{1, \dots, N\}$ via dimension tree
 - 6: **for** $n \in \{1, \dots, N\}$ **do**
 - 7: $\mathbf{A}_p^{(n)} \leftarrow \mathbf{A}^{(n)}, d\mathbf{A}^{(n)} \leftarrow \mathbf{O}$
 - 8: **end for**
 - 9: **while** $\sum_{i=1}^N \|\mathbf{G}^{(i)}\|_F > \varepsilon$ and $\forall i \in \{1, \dots, N\}, \|d\mathbf{A}^{(i)}\|_F < \epsilon$ **do**
 - 10: **for** $n \in \{1, \dots, N\}$ **do**
 - 11: $\mathbf{\Gamma}^{(n)} \leftarrow \mathbf{S}^{(1)} * \dots * \mathbf{S}^{(n-1)} * \mathbf{S}^{(n+1)} * \dots * \mathbf{S}^{(N)}$
 - 12: $\tilde{\mathbf{M}}^{(n)}(y, k) = \mathbf{M}_p^{(n)}(y, k) + \sum_{i=1, i \neq n}^N \sum_{x=1}^{s_i} \mathcal{M}_p^{(i, n)}(x, y, k) d\mathbf{A}^{(i)}(x, k)$
 - 13: $\mathbf{A}_{\text{new}}^{(n)} \leftarrow \tilde{\mathbf{M}}^{(n)} \mathbf{\Gamma}^{(n)\dagger}$
 - 14: $\mathbf{G}^{(n)} \leftarrow (\mathbf{A}^{(n)} - \mathbf{A}_{\text{new}}^{(n)}) \mathbf{\Gamma}^{(n)}$
 - 15: $\mathbf{A}^{(n)} \leftarrow \mathbf{A}_{\text{new}}^{(n)}$
 - 16: $\mathbf{S}^{(n)} \leftarrow \mathbf{A}^{(n)T} \mathbf{A}^{(n)}$
 - 17: $d\mathbf{A}^{(n)} = \mathbf{A}_{\text{new}}^{(n)} - \mathbf{A}_p^{(n)}$
 - 18: **end for**
 - 19: **end while**
 - 20: **end if**
 - 21: Perform regular ALS sweep as in Algorithm 2.1, taking $d\mathbf{A}^{(n)} \leftarrow \mathbf{A}_{\text{new}}^{(n)} - \mathbf{A}^{(n)}$ for each $n \in \{1, \dots, N\}$
 - 22: **end while**
 - 23: **return** $[\mathbf{A}^{(1)}, \dots, \mathbf{A}^{(N)}]$
-

4.2. Tucker-ALS. We derive a similar pairwise perturbation algorithm for Tucker ALS. We now seek to approximate $\tilde{\mathbf{Y}}^{(n)} \approx \mathbf{Y}^{(n)}$ (defined in Section 2.3), by forming and reusing pairwise perturbation operators, which are special cases of the following TTMc intermediates.

DEFINITION 4.2. $\mathcal{Y}^{(i_1, i_2, \dots, i_m)}$ is defined as follows,

$$\mathcal{Y}^{(i_1, i_2, \dots, i_m)} = \mathcal{X} \times_{j \in \{1, \dots, N\} \setminus \{i_1, i_2, \dots, i_m\}} \mathbf{A}^{(j)T}.$$

Where \mathcal{X} is contracted with all the matrices $\mathbf{A}^{(j)}$ without $\mathbf{A}^{(i_1)}, \dots, \mathbf{A}^{(i_m)}$.

Similar to the expression for $\mathbf{M}^{(n)}$ in CP-ALS, $\mathcal{Y}^{(n)}$ can be expressed as

$$\mathcal{Y}^{(n)} = \mathcal{X} \times_{i=1, i \neq n}^N (\mathbf{A}_p^{(i)T} + d\mathbf{A}^{(i)T}).$$

The expression above can be rewritten as a function of $\mathcal{Y}_p^{(i_1, i_2, \dots, i_m)}$, which is defined in the same way as $\mathcal{Y}^{(i_1, i_2, \dots, i_m)}$ except that \mathcal{X} is contracted with $\mathbf{A}_p^{(j)}$ for $\mathcal{Y}_p^{(i_1, i_2, \dots, i_m)}$,

$$\mathcal{Y}^{(n)} = \mathcal{Y}_p^{(n)} + \sum_{i=1, i \neq n}^N \mathcal{Y}_p^{(i, n)} \times_i d\mathbf{A}^{(i)T} + \sum_{i=1, i \neq n}^N \sum_{j=i+1, j \neq n}^N \mathcal{Y}_p^{(i, j, n)} \times_i d\mathbf{A}^{(i)T} \times_j d\mathbf{A}^{(j)T} + \dots.$$

The pairwise perturbation again takes only the first order terms in $d\mathbf{A}^{(i)}$, computing

$$\tilde{\mathcal{Y}}^{(n)} = \mathcal{Y}_p^{(n)} + \sum_{i=1, i \neq n}^N \mathcal{Y}_p^{(i, n)} \times_i d\mathbf{A}^{(i)T},$$

$$\text{where } \mathcal{Y}_p^{(n)} = \mathcal{X} \times_{l=1, l \neq n}^N \mathbf{A}_p^{(l)T}, \quad \text{and } \mathcal{Y}_p^{(i, n)} = \mathcal{X} \times_{j \in \{1, \dots, N\} \setminus \{i, n\}} \mathbf{A}_p^{(j)T}.$$

Given $\mathcal{Y}_p^{(i, n)}$ and $\mathcal{Y}_p^{(n)}$, $\tilde{\mathcal{Y}}^{(n)}$ for $n \in \{1, \dots, N\}$ can be calculated with $2Ns^2R^{N-1}$ cost overall. In Section 5.2, we show that the relative Frobenius norm approximation error of $\tilde{\mathcal{Y}}^{(n)}$ with respect to $\mathcal{Y}^{(n)}$ is small, so long as each $\frac{\|d\mathbf{A}^{(n)}\|_F}{\|\mathbf{A}^{(n)}\|_F}$ is sufficiently small. Algorithm 4.2 presents the PP-Tucker-ALS method described above.

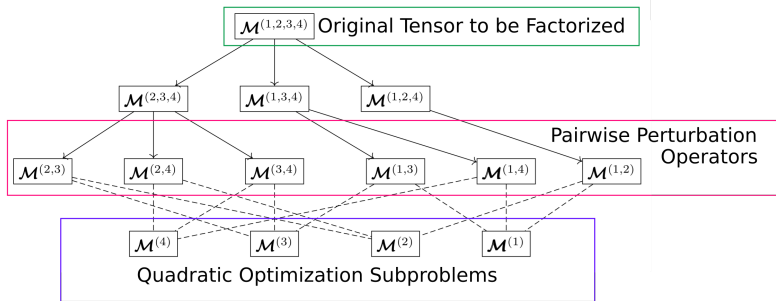


FIGURE 1. Dimension tree for construction of pairwise perturbation operators $N = 4$.

4.3. Dimension Trees for Pairwise Perturbation Operators. Computation of the pairwise perturbation operators $\mathcal{M}_p^{(i, n)}$ and of $\mathcal{M}_p^{(n)}$ can benefit from amortization of common tensor contraction (Khatri-Rao product or tensor-times-matrix product) subexpressions. In the context of ALS, this technique is known as dimension trees [6, 29, 41, 48] and has been successfully employed to accelerate TTMC

Algorithm 4.2 Tucker_ALS_PP: Pairwise perturbation procedure for Tucker-ALS

```

1: Input: tensor  $\mathcal{X} \in \mathbb{R}^{\prod_{i=1}^N s_i}$ , decomposition ranks  $\{R_1, \dots, R_N\}$ , stopping criteria  $\varepsilon$ , PP
   tolerance  $\epsilon$ 
2: Initialize  $[\mathcal{G}; \mathbf{A}^{(1)}, \dots, \mathbf{A}^{(N)}]$  using HOSVD
3: while  $\|\mathcal{F}\|_F > \varepsilon$  do
4:   if  $\forall i \in \{1, \dots, N\}, \|d\mathbf{A}^{(i)}\|_F < \epsilon$  then
5:     Compute  $\mathcal{Y}_p^{(i,n)}, \mathcal{Y}_p^{(n)}$  for  $i, n \in \{1, \dots, N\}$  via dimension tree
6:     for  $n \in \{1, \dots, N\}$  do
7:        $\mathbf{A}_p^{(n)} \leftarrow \mathbf{A}^{(n)}, d\mathbf{A}^{(n)} \leftarrow \mathbf{O}$ 
8:     end for
9:     while  $\|\mathcal{F}\|_F > \varepsilon$  and  $\forall i \in \{1, \dots, N\}, \|d\mathbf{A}^{(i)}\|_F < \epsilon$  do
10:      for  $n \in \{1, \dots, N\}$  do
11:         $\mathcal{Y} \leftarrow \mathcal{Y}_p^{(n)} + \sum_{i=1, i \neq n}^N \mathcal{Y}_p^{(i,n)} \times_i d\mathbf{A}^{(i)}$ 
12:         $\mathbf{A}^{(n)} \leftarrow R_n$  leading left singular vectors of  $\mathbf{Y}_{(n)}$ 
13:         $d\mathbf{A}^{(n)} \leftarrow \mathbf{A}^{(n)} - \mathbf{A}_p^{(n)}$ 
14:         $\mathcal{G}_{\text{new}} \leftarrow \mathcal{X} \times_1 \mathbf{A}^{(1)T} \dots \times_N \mathbf{A}^{(N)T}$ 
15:         $\mathcal{F} \leftarrow \mathcal{G}_{\text{new}} - \mathcal{G}$ 
16:         $\mathcal{G} \leftarrow \mathcal{G}_{\text{new}}$ 
17:      end for
18:    end while
19:   end if
20:   Perform regular ALS sweep as in Algorithm 2.3, taking  $d\mathbf{A}^{(n)} \leftarrow \mathbf{A}_{\text{new}}^{(n)} - \mathbf{A}^{(n)}$  for each
      $n \in \{1, \dots, N\}$ 
21: end while
22: return  $[\mathcal{G}; \mathbf{A}^{(1)}, \dots, \mathbf{A}^{(N)}]$ 

```

and MTTKRP. The same trees can be used for both CP and Tucker, although the tensor intermediates and contraction operations are different (Khatri-Rao products for CP and tensor times matrix products for Tucker). We describe the trees for CP decomposition, computing each $\mathcal{M}_p^{(i,n)}$ and $\mathcal{M}_p^{(n)}$. Figure 1 describes the dimension tree for $N = 4$ plus an additional level for computation of the $\mathcal{M}_p^{(n)}$ matrices. Our tree constructions assume that the tensors are equidimensional, if this is not the case, the largest dimensions should be contracted first.

The main goal of the dimension tree is to perform a minimal number of contractions to obtain each $\mathcal{M}_p^{(i,n)}$. Each matrix $\mathcal{M}_p^{(n)}$ can be simply obtained by a contraction with $\mathcal{M}_p^{(i,n)}$ for any $i \neq n$. Each level of the tree for $l = 1, \dots, N - 1$ should contain intermediate tensors containing $N - l + 1$ uncontracted modes belonging to the original tensor (the root is the original tensor $\mathcal{X} = \mathcal{M}^{(1, \dots, N)}$). It is necessary to maintain the invariant that for any pair of the original tensor modes, each level should contain an intermediate for which these modes are uncontracted. Since the leaves at level $l = N - 1$ have two uncontracted modes, they will include each $\mathcal{M}_p^{(i,n)}$ for $i < n$ ($\mathcal{M}_p^{(i,n)} = \mathcal{M}_p^{(n,i)T}$). At level l it then suffices to compute $\binom{l+1}{2}$ tensors $\mathcal{M}^{(i,j,l+3,l+4, \dots, N)}$, $\forall i, j \in \{1, \dots, l+2\}, i < j$. Each $\mathcal{M}^{(i,j,l+3,l+4, \dots, N)}$ can be computed by contraction of $\mathcal{M}^{(s,t,v,l+3,l+4, \dots, N)}$ and $\mathbf{A}^{(w)}$ where $\{s, t, v\} = \{i, j, w\}$ with $w = \max_{w \in \{l, \dots, l+2\} \setminus \{i, j\}}(w)$ and $s < t < v$.

The construction of pairwise perturbation operators for CP decomposition costs

$$2R \sum_{l=2}^{N-1} \binom{l+1}{2} s^{N-l+2} = 6s^N R + 12s^{N-1} R + O(s^{N-2} R^2).$$

The cost to form pairwise perturbation operators for Tucker decomposition is

$$2 \sum_{l=2}^{N-1} \binom{l+1}{2} s^{N-l+2} R^{l-1} = 6s^N R + 12s^{N-1} R^2 + O(s^{N-2} R^3).$$

5. Error Analysis. In this section, we formally bound the approximation error of the pairwise perturbation algorithm relative to standard ALS, leveraging the tensor condition number notion introduced in Section 3. We show that quadratic optimization problems computed by pairwise perturbation differ only slightly from ALS so long as the factor matrices have not changed significantly since the construction of the pairwise perturbation operators.

We summarize the CP and Tucker error pairwise perturbation error bounds in Table 2. For CP decomposition, we obtain condition-number-dependent column-wise error bounds on $\mathbf{M}^{(n)}$ (the right-hand sides in the linear least squares subproblems), based on the magnitude of the relative perturbation to $\mathbf{A}^{(n)}$ since the formation of the pairwise perturbation operators. For Tucker decomposition, we again obtain bounds based on the perturbation to $\mathbf{A}^{(n)}$, this time for $\mathbf{Y}^{(n)}$ (the tensors on whose matricizations a truncated SVD is performed). For Tucker decomposition, we obtain stronger results showing error bounds that are independent of the tensor condition number, which assume that either the residual of the Tucker decomposition is bounded (it suffices that the decomposition achieves one digit of accuracy in residual) or that the ratio of rank to dimension is not too large.

TABLE 2

Error bound comparison for pairwise perturbation algorithm between CP decomposition and Tucker decomposition. It is worth noting that for the left two columns in the Table, the input tensor needs to have same length in each mode. \mathcal{R} is the residual of Tucker decomposition.

	$\mathcal{X} \in \mathbb{R}^{\otimes_{i=1}^N s}$ $\frac{\ d\mathbf{a}_k^{(n)}\ _2}{\ \mathbf{a}_k^{(n)}\ _2} \leq \epsilon$	$\mathcal{X} \in \mathbb{R}^{\otimes_{i=1}^N s}$ $\ d\mathbf{A}^{(n)}\ _2 \leq \epsilon$	$\mathcal{X} \in \mathbb{R}^{\otimes_{i=1}^N s_i}$ $\ d\mathbf{A}^{(n)}\ _2 \leq \epsilon$ $\ \mathcal{R}\ _2 \leq \frac{1}{3}\ \mathcal{X}\ _2$	$\mathcal{X} \in \mathbb{R}^{\otimes_{i=1}^N s_i}$ $\ d\mathbf{A}^{(n)}\ _F \leq \epsilon$
CP	$\frac{\ \tilde{\mathbf{m}}_k^{(n)} - \mathbf{m}_k^{(n)}\ _2}{\ \mathbf{m}_k^{(n)}\ _2} = O(\epsilon^2 \kappa(\mathcal{X}))$	No clear bound	No clear bound	No clear bound
Tucker	$\frac{\ \tilde{\mathbf{Y}}^{(n)}(:,t) - \mathbf{Y}^{(n)}(:,t)\ _2}{\ \mathbf{Y}^{(n)}(:,t)\ _2} = O(\epsilon^2 \kappa(\mathcal{X}))$	$\frac{\ \tilde{\mathbf{Y}}^{(n)} - \mathbf{Y}^{(n)}\ _2}{\ \mathbf{Y}^{(n)}\ _2} = O(\epsilon^2 \kappa(\mathcal{X}))$	$\frac{\ \tilde{\mathbf{Y}}^{(n)} - \mathbf{Y}^{(n)}\ _2}{\ \mathbf{Y}^{(n)}\ _2} = O(\epsilon^2)$	$\frac{\ \tilde{\mathbf{Y}}^{(n)} - \mathbf{Y}^{(n)}\ _F}{\ \mathbf{Y}^{(n)}\ _F} = O(\epsilon^2 (\frac{s}{R})^{N/2})$

5.1. CP-ALS. Using Lemma 3.1, we prove in Theorem 5.1 that when the column-wise norm of $d\mathbf{A}^{(n)} = \mathbf{A}^{(n)} - \mathbf{A}_p^{(n)}$ relative to the norm of $\mathbf{A}^{(n)}$, for $n \in \{1, \dots, N\}$, is small and the number of rows in $\mathbf{M}^{(n)}$ is larger or equal to the length of other tensor modes, the column-wise relative error for $\mathbf{M}^{(n)}$ with respect to exact ALS with the factor matrices $\mathbf{A}^{(n)}$, for $n \in \{1, \dots, N\}$, is also small.

THEOREM 5.1. *If $\frac{\|d\mathbf{a}_k^{(n)}\|_2}{\|\mathbf{a}_k^{(n)}\|_2} \leq \epsilon \ll 1$ for $n \in \{1, \dots, N\}, k \in \{1, \dots, R\}$ and $s_m \leq s_n$ for any $m \in \{1, \dots, N\}$, the pairwise perturbation algorithm computes $\tilde{\mathbf{M}}^{(n)}$ with column-wise error,*

$$\frac{\|\tilde{\mathbf{m}}_k^{(n)} - \mathbf{m}_k^{(n)}\|_2}{\|\mathbf{m}_k^{(n)}\|_2} = O(\epsilon^2 \kappa(\mathcal{X})),$$

where $\mathbf{M}^{(n)}$ is the matrix given by a regular ALS iteration.

Proof. We bound the error due to second order perturbations in $d\mathbf{A}^{(1)}, \dots, d\mathbf{A}^{(n)}$, by similar analysis, higher-order perturbations would lead to errors smaller by a factor of $O(\text{poly}(N)\epsilon)$ and are consequently negligible if $\epsilon \ll 1$. Consider the order four tensors $\mathcal{M}^{(i,j,n)}$ (Definition 4.1) based on the current factor matrices $\mathbf{A}^{(1)}, \dots, \mathbf{A}^{(N)}$ and the pairwise perturbation operators $\mathcal{M}_p^{(i,j,n)}$ based on past factor matrices $\mathbf{A}_p^{(1)}, \dots, \mathbf{A}_p^{(N)}$. The contribution of second order terms to the error is

$$\tilde{\mathbf{m}}_k^{(n)}(x) - \mathbf{m}_k^{(n)}(x) \approx \sum_{\substack{i,j \in \{1, \dots, n-1, n+1, \dots, N\} \\ i \neq j}} \sum_{y=1}^s \sum_{z=1}^s \mathcal{M}_p^{(i,j,n)}(x, y, z, k) d\mathbf{a}_k^{(i)}(y) d\mathbf{a}_k^{(j)}(z).$$

This absolute error has magnitude,

$$\|\tilde{\mathbf{m}}_k^{(n)} - \mathbf{m}_k^{(n)}\|_2 \leq \binom{N}{2} \max_{i,j} \|\mathcal{M}_p^{(i,j,n)}(\cdot, \cdot, \cdot, k)\|_2 \|d\mathbf{a}_k^{(i)}\|_2 \|d\mathbf{a}_k^{(j)}\|_2.$$

Using the fact that for any i, j we can express $\mathbf{m}_k^{(n)}$ as

$$\mathbf{m}_k^{(n)}(x) = \sum_{y=1}^s \sum_{z=1}^s \mathcal{M}^{(i,j,n)}(x, y, z, k) \mathbf{a}_k^{(i)}(y) \mathbf{a}_k^{(j)}(z),$$

we can lower bound the magnitude of the answer with respect to any $\mathcal{M}^{(i,j,n)}$,

$$\|\mathbf{m}_k^{(n)}\|_2 \geq \inf\{\|\mathbf{f}_{\mathcal{M}^{(i,j,n)}(\cdot, \cdot, \cdot, k)}\|_2\} \|\mathbf{a}_k^{(i)}\|_2 \|\mathbf{a}_k^{(j)}\|_2.$$

Combining the upper bound on the absolute error with the lower bound on norm,

$$\frac{\|\tilde{\mathbf{m}}_k^{(n)} - \mathbf{m}_k^{(n)}\|_2}{\|\mathbf{m}_k^{(n)}\|_2} \leq \binom{N}{2} \max_{i,j} \frac{\|\mathcal{M}_p^{(i,j,n)}(\cdot, \cdot, \cdot, k)\|_2 \|d\mathbf{a}_k^{(i)}\|_2 \|d\mathbf{a}_k^{(j)}\|_2}{\inf\{\|\mathbf{f}_{\mathcal{M}^{(i,j,n)}(\cdot, \cdot, \cdot, k)}\|_2\} \|\mathbf{a}_k^{(i)}\|_2 \|\mathbf{a}_k^{(j)}\|_2}.$$

Lemma 3.1 implies that for any i, j, k ,

$$\|\mathcal{M}_p^{(i,j,n)}(\cdot, \cdot, \cdot, k)\|_2 \leq \|\mathcal{X}\|_2 \prod_{l \in \{1, \dots, N\} \setminus \{i, j, n\}} \|\mathbf{A}_p^{(l)}(\cdot, k)\|_2$$

and that

$$\inf\{\|\mathbf{f}_{\mathcal{M}^{(i,j,n)}(\cdot, \cdot, \cdot, k)}\|_2\} \geq \inf\{\|\mathbf{f}_{\mathcal{X}}\|_2\} \prod_{l \in \{1, \dots, N\} \setminus \{i, j, n\}} \|\mathbf{A}^{(l)}(\cdot, k)\|_2.$$

Since, $\|\mathbf{A}_p^{(l)}(\cdot, k)\|_2 \leq (1 + \epsilon) \|\mathbf{A}^{(l)}(\cdot, k)\|_2$, we obtain the bound,

$$\frac{\|\tilde{\mathbf{m}}_k^{(n)} - \mathbf{m}_k^{(n)}\|_2}{\|\mathbf{m}_k^{(n)}\|_2} \leq \binom{N}{2} \kappa(\mathcal{X}) (1 + \epsilon)^{N-3} \epsilon^2 \approx \binom{N}{2} \kappa(\mathcal{X}) \epsilon^2. \quad \square$$

This error bound is relative to the condition number of \mathcal{X} , which means the bound is sensitive to the input tensor and that the error may be unbounded if \mathcal{X} has an exact CP decomposition of rank at most $\min_i s_i$.

5.2. Tucker-ALS. For Tucker decomposition, the pairwise perturbation approximation satisfies even better bounds than for CP decomposition, due to the orthogonality of the factor matrices. We demonstrate that

- for TTMC, the same relative error bound as for MTTKRP holds when the 2-norm relative perturbations of the input matrices are bounded by $O(\epsilon)$ (Theorem 5.4),
- the error satisfies a condition-number-independent bound of $O(\epsilon^2)$, so long as the residual of Tucker decomposition is small (Theorem 5.5),
- the relative error is bounded in Frobenius norm by $O(\epsilon^2)$ for a fixed problem size (Theorem 5.8).

Using Lemma 3.1, we prove in Lemma 5.2 that after contracting a tensor with a matrix with orthonormal rows, whose row length is higher or equal to the column length, the contracted tensor norm is the same as the original tensor norm.

LEMMA 5.2. *Given tensor $\mathcal{G} \in \mathbb{R}^{\otimes_{i=1}^N r_i}$, the mode- n product for any $n \in \{1, \dots, N\}$, with a matrix with orthonormal columns $\mathbf{M} \in \mathbb{R}^{s \times r_n}$, $r_n \leq s$, satisfies $\|\mathcal{G}\|_2 = \|\mathcal{G} \times_n \mathbf{M}\|_2$.*

Proof. Based on the submultiplicative property of the tensor norm (Lemma 3.1),

$$\|\mathcal{G}\|_2 = \|\mathcal{G} \times_n (\mathbf{M}^T \mathbf{M})\|_2 = \|\mathcal{G} \times_n \mathbf{M} \times_n \mathbf{M}^T\|_2 \leq \|\mathcal{G} \times_n \mathbf{M}\|_2 \|\mathbf{M}^T\|_2 \leq \|\mathcal{G} \times_n \mathbf{M}\|_2,$$

and simultaneously, $\|\mathcal{G} \times_n \mathbf{M}\|_2 \leq \|\mathcal{G}\|_2 \|\mathbf{M}\|_2 \leq \|\mathcal{G}\|_2$. \square

Similar to Theorem 5.1, we show in Theorem 5.3 that in Tucker decomposition of equidimensional tensors if the column-wise perturbation of the matrices $\mathbf{A}^{(n)}$ for $n \in \{1, \dots, N\}$ with respect to those used to construct the pairwise perturbation operators is small, the column-wise relative error for the $\mathbf{Y}_{(n)}^{(n)}$ is also small with respect to what would be computed by regular ALS given the same factor matrices and core tensor.

THEOREM 5.3. *For $\mathcal{X} \in \mathbb{R}^{\otimes_{i=1}^N s}$, if $\|\mathbf{d}\mathbf{a}_k^{(n)}\|_2 \leq \epsilon \ll 1$ for $n \in \{1, \dots, N\}, k \in \{1, \dots, R\}$, the pairwise perturbation algorithm computes $\tilde{\mathcal{Y}}^{(n)}$ with error, for $t \in \{1, \dots, R^{N-1}\}$,*

$$\frac{\|\tilde{\mathbf{Y}}_{(n)}^{(n)}(:, t) - \mathbf{Y}_{(n)}^{(n)}(:, t)\|_2}{\|\mathbf{Y}_{(n)}^{(n)}(:, t)\|_2} = O(\epsilon^2 \kappa(\mathcal{X})),$$

where $\tilde{\mathbf{Y}}_{(n)}^{(n)}, \mathbf{Y}_{(n)}^{(n)}$ are the mode- n matricizations of $\tilde{\mathcal{Y}}^{(n)}, \mathcal{Y}^{(n)}$, respectively.

We omit the proof of Theorem 5.3 as it differs little from that of Theorem 5.1,

- each column of $\mathbf{Y}_{(n)}^{(n)}(:, t)$ is obtained by contraction of a column of each of the $\mathbf{A}^{(i)}$ matrices for $i \neq n$ and the tensor \mathcal{X} ,
- the portion of the Tucker pairwise perturbation operator used to obtain the approximation is also a contraction of \mathcal{X} with $N - 3$ vectors.

Using Lemma 3.1, we prove in Theorem 5.4 that when the tensor has same length in each mode and the relative error of the matrices $\mathbf{A}^{(n)}$ for $n \in \{1, \dots, N\}$ is small, the relative error for the $\tilde{\mathcal{Y}}^{(n)}$ is also small.

THEOREM 5.4. *Given tensor $\mathcal{X} \in \mathbb{R}^{\otimes_{i=1}^N s}$, if $\|\mathbf{d}\mathbf{A}^{(n)}\|_2 \leq \epsilon \ll 1$ for $n \in \{1, \dots, N\}$, $\tilde{\mathcal{Y}}^{(n)}$ is constructed with error,*

$$\frac{\|\tilde{\mathcal{Y}}^{(n)} - \mathcal{Y}^{(n)}\|_2}{\|\mathcal{Y}^{(n)}\|_2} = O(\epsilon^2 \kappa(\mathcal{X})).$$

Proof. As in Theorem 5.1, we bound the error due to second-order terms,

$$\frac{\|\tilde{\mathcal{Y}}^{(n)} - \mathcal{Y}^{(n)}\|_2}{\|\mathcal{Y}^{(n)}\|_2} = \binom{N}{2} \max_{i,j} \frac{\|\mathcal{Y}_p^{(i,j,n)} \times_i d\mathbf{A}^{(i)T} \times_j d\mathbf{A}^{(j)T}\|_2}{\|\mathcal{Y}^{(i,j,n)} \times_i \mathbf{A}^{(i)T} \times_j \mathbf{A}^{(j)T}\|_2}.$$

From Lemma 3.1, we have

$$\frac{\|\mathcal{Y}_p^{(i,j,n)} \times_i d\mathbf{A}^{(i)T} \times_j d\mathbf{A}^{(j)T}\|_2}{\|\mathcal{Y}^{(i,j,n)} \times_i \mathbf{A}^{(i)T} \times_j \mathbf{A}^{(j)T}\|_2} \leq \frac{\|\mathcal{Y}_p^{(i,j,n)}\|_2 \|d\mathbf{A}^{(i)}\|_2 \|d\mathbf{A}^{(j)}\|_2}{\inf\{\|\mathbf{f}_{\mathcal{Y}^{(i,j,n)}}\|_2\} \|\mathbf{A}^{(i)}\|_2 \|\mathbf{A}^{(j)}\|_2}.$$

Since $\mathbf{A}^{(i)}$ and $\mathbf{A}^{(j)}$ are both matrices with orthonormal columns,

$$\frac{\|\tilde{\mathcal{Y}}^{(n)} - \mathcal{Y}^{(n)}\|_F}{\|\mathcal{Y}^{(n)}\|_F} \leq \binom{N}{2} \max_{i,j} \frac{\|\mathcal{Y}_p^{(i,j,n)}\|_2 \|d\mathbf{A}^{(i)}\|_2 \|d\mathbf{A}^{(j)}\|_2}{\inf\{\|\mathbf{f}_{\mathcal{Y}^{(i,j,n)}}\|_2\}} = O(\epsilon^2 \kappa(\mathcal{X})). \quad \square$$

Using Lemma 5.2, we prove in Theorem 5.5 that when the relative error of the matrices $\mathbf{A}^{(n)}$ for $n \in \{1, \dots, N\}$ is small and the residual of the Tucker decomposition is loosely bounded, the relative error bound for the $\mathcal{Y}^{(n)}$ is independent of the condition number of the input tensor.

THEOREM 5.5. *Given tensor $\mathcal{X} \in \mathbb{R}^{\otimes_{i=1}^N s_i}$, if $\|d\mathbf{A}^{(n)}\|_2 \leq \epsilon \ll 1$ for $n \in \{1, \dots, N\}$ and $\|\mathcal{X} - \llbracket \mathcal{G}; \mathbf{A}^{(1)}, \mathbf{A}^{(2)}, \dots, \mathbf{A}^{(N)} \rrbracket\|_2 \leq \frac{1}{3} \|\mathcal{X}\|_2$, $\tilde{\mathcal{Y}}^{(n)}$ is constructed with error,*

$$\frac{\|\tilde{\mathcal{Y}}^{(n)} - \mathcal{Y}^{(n)}\|_2}{\|\mathcal{Y}^{(n)}\|_2} = O(\epsilon^2).$$

Proof.

$$\begin{aligned} \frac{\|\tilde{\mathcal{Y}}^{(n)} - \mathcal{Y}^{(n)}\|_2}{\|\mathcal{Y}^{(n)}\|_2} &= \binom{N}{2} \max_{i,j} \frac{\|\mathcal{Y}_p^{(i,j,n)} \times_i d\mathbf{A}^{(i)T} \times_j d\mathbf{A}^{(j)T}\|_2}{\|\mathcal{Y}^{(n)}\|_2} \\ &\leq \binom{N}{2} \max_{i,j} \frac{\|\mathcal{Y}_p^{(i,j,n)}\|_2 \|d\mathbf{A}^{(i)}\|_2 \|d\mathbf{A}^{(j)}\|_2}{\|\mathcal{Y}^{(n)}\|_2}. \end{aligned}$$

Let $\tilde{\mathcal{X}} = \llbracket \mathcal{G}; \mathbf{A}^{(1)}, \mathbf{A}^{(2)}, \dots, \mathbf{A}^{(N)} \rrbracket$, $\mathcal{R} = \mathcal{X} - \tilde{\mathcal{X}}$. Define the tensors $\mathcal{Z}^{(i,j,n)}$ by contraction of \mathcal{R} with all except three factor matrices,

$$\mathcal{Z}^{(i,j,n)} = \mathcal{R} \quad \times \quad \mathbf{A}^{(r)T},$$

$$r \in \{1, \dots, N\} \setminus \{i, j, n\}$$

For $\|\mathcal{X} - \tilde{\mathcal{X}}\|_2 = \|\mathcal{R}\|_2 \leq \frac{1}{3} \|\mathcal{X}\|_2$, we have $\frac{2}{3} \|\mathcal{X}\|_2 \leq \|\tilde{\mathcal{X}}\|_2 \leq \frac{4}{3} \|\mathcal{X}\|_2$. Based on Lemma 5.2,

$$\begin{aligned} \|\mathcal{Y}^{(n)}\|_2 &= \|\mathcal{G} \times_n \mathbf{A}^{(n)} + \mathcal{Z}^{(i,j,n)} \times_i \mathbf{A}^{(i)T} \times_j \mathbf{A}^{(j)T}\|_2 \\ &\geq \|\mathcal{G}\|_2 - \|\mathcal{Z}^{(i,j,n)}\|_2 \|\mathbf{A}^{(i)T}\|_2 \|\mathbf{A}^{(j)T}\|_2 \geq \|\mathcal{G}\|_2 - \|\mathcal{R}\|_2 \geq \frac{1}{3} \|\mathcal{X}\|_2, \end{aligned}$$

Additionally,

$$\|\mathcal{Y}^{(i,j,n)}\|_2 = \|\mathcal{G} \times_i \mathbf{A}^{(i)} \times_j \mathbf{A}^{(j)} \times_n \mathbf{A}^{(n)} + \mathcal{Z}^{(i,j,n)}\|_2 \leq \|\mathcal{G}\|_2 + \|\mathcal{R}\|_2 \leq \frac{5}{3} \|\mathcal{X}\|_2.$$

Therefore,

$$\frac{\|\tilde{\mathcal{Y}}^{(n)} - \mathcal{Y}^{(n)}\|_2}{\|\mathcal{Y}^{(n)}\|_2} \leq \binom{N}{2} \max_{i,j} \frac{\|\mathcal{Y}_p^{(i,j,n)}\|_2 \|d\mathbf{A}^{(i)}\|_2 \|d\mathbf{A}^{(j)}\|_2}{\|\mathcal{Y}^{(n)}\|_2} \leq \binom{N}{2} \frac{\frac{5}{3} \|\mathcal{X}\|_2 \epsilon^2}{\frac{1}{3} \|\mathcal{X}\|_2} = O(\epsilon^2). \quad \square$$

We now derive a Frobenius norm error bound that is independent of residual norm and tensor condition number, but is looser based on a power the ratio of the tensor dimensions and the Tucker rank. We arrive at this result (Theorem 5.8) by obtaining a lower bound on the residual achieved by the HOSVD (Lemmas 5.6 and 5.7).

LEMMA 5.6. *Given tensor $\mathcal{X} \in \mathbb{R}^{\otimes_{i=1}^N s_i}$ and matrix $\mathbf{A} \in \mathbb{R}^{R \times s_n}$, where $R < s_n$ and \mathbf{A} consists of R leading left singular vectors of $\mathbf{X}_{(n)}$. Let $\mathcal{G} = \mathcal{X} \times_n \mathbf{A}$, $\|\mathcal{X}\|_F \geq \|\mathcal{G}\|_F \geq \sqrt{\frac{R}{s_n}} \|\mathcal{X}\|_F$.*

Proof. The singular values of $\mathbf{A}\mathbf{X}_{(n)}$ are the first R singular values of $\mathbf{X}_{(n)}$. Since the square of the Frobenius norm of a matrix is the sum of the squares of the singular values, $\|\mathcal{G}\|_F^2 = \|\mathbf{A}\mathbf{X}_{(n)}\|_F^2 \geq (R/s_n)\|\mathbf{X}_{(n)}\|_F^2 = (R/s_n)\|\mathcal{X}\|_F^2$ and $\|\mathcal{G}\|_F \leq \|\mathcal{X}\|_F$. \square

LEMMA 5.7. *For any $\mathcal{X} \in \mathbb{R}^{\otimes_{i=1}^N s}$, $\|\mathcal{Y}^{(n)}\|_F \geq (\frac{R}{s})^{N/2} \|\mathcal{X}\|_F$ if Tucker-ALS starts from an interlaced HOSVD.*

Proof. In Tucker-ALS, $\|\mathcal{G}\|_F$ is strictly increasing after each Tucker iteration, where \mathcal{G} is \mathcal{X} 's HOSVD core tensor. Since the interlaced SVD computes each $\mathbf{A}^{(n)}$ from the truncated SVD of the product of \mathcal{X} and the first $n-1$ factor matrices, we can apply Lemma 5.6 N times,

$$\begin{aligned} \|\mathcal{X} \times_1 \mathbf{A}^{(1)T} \cdots \times_{N-1} \mathbf{A}^{(N-1)T}\|_F &\geq \|\mathcal{G}\|_F \geq \sqrt{\frac{R}{s}} \|\mathcal{X} \times_1 \mathbf{A}^{(1)T} \cdots \times_{N-1} \mathbf{A}^{(N-1)T}\|_F \\ &\vdots \\ \|\mathcal{X}\|_F &\geq \|\mathcal{G}\|_F \geq (R/s)^{N/2} \|\mathcal{X}\|_F. \quad \square \end{aligned}$$

THEOREM 5.8. *Given tensor $\mathcal{X} \in \mathbb{R}^{\otimes_{i=1}^N s}$, if $\|d\mathbf{A}^{(n)}\|_F \leq \epsilon$ for $n \in [1, N]$, $\tilde{\mathcal{Y}}^{(n)}$ is constructed with error,*

$$\frac{\|\tilde{\mathcal{Y}}^{(n)} - \mathcal{Y}^{(n)}\|_F}{\|\mathcal{Y}^{(n)}\|_F} = O\left(\epsilon^2 \left(\frac{s}{R}\right)^{N/2}\right).$$

Proof.

$$\frac{\|\tilde{\mathcal{Y}}^{(n)} - \mathcal{Y}^{(n)}\|_F}{\|\mathcal{Y}^{(n)}\|_F} = \binom{N}{2} \max_{i,j} \frac{\|\mathcal{Y}_p^{(i,j,n)} \times_i d\mathbf{A}^{(i)T} \times_j d\mathbf{A}^{(j)T}\|_F}{\|\mathcal{Y}^{(n)}\|_F}.$$

From Lemma 5.7, we have

$$\frac{\|\mathcal{Y}_p^{(i,j,n)} \times_i d\mathbf{A}^{(i)T} \times_j d\mathbf{A}^{(j)T}\|_F}{\|\mathcal{Y}^{(n)}\|_F} \leq \frac{\|\mathcal{X}\|_F \|d\mathbf{A}^{(i)}\|_F \|d\mathbf{A}^{(j)}\|_F}{(\frac{R}{s})^{N/2} \|\mathcal{X}\|_F}.$$

Consequently, we can bound the relative error by

$$\frac{\|\tilde{\mathcal{Y}}^{(n)} - \mathcal{Y}^{(n)}\|_F}{\|\mathcal{Y}^{(n)}\|_F} \leq \binom{N}{2} (s/R)^{N/2} \max_{i,j} \|d\mathbf{A}^{(i)}\|_F \|d\mathbf{A}^{(j)}\|_F = O\left(\epsilon^2 \left(\frac{s}{R}\right)^{N/2}\right). \quad \square$$

6. Experiments. We evaluate the performance of the pairwise perturbation algorithms on both synthetic and application datasets. The synthetic experiments enable us to test tensors with known factors and to measure whether the algorithm works. We also consider publicly available tensor datasets and demonstrate the effectiveness of our algorithms on practical problems.

We compare the performance of our own implementations of regular ALS with dimension trees and the pairwise perturbation algorithms.¹ All codes are implemented in C++ using Cyclops Tensor Framework (v1.5.3) [44] for all contractions and leveraging its wrapper for the ScaLAPACK [9] SVD routine. Cyclops is a distributed-memory library for tensor contractions, which leverages MPI for interprocess communication and OpenMP for threading. Cyclops employs the HPTT library [45] for high-performance local transposition.

The performance results are collected on the Stampede2 supercomputer Texas Advanced Computing Center located at the University of Texas at Austin. We leverage the Knight’s Landing (KNL) nodes exclusively, each of which consists of 68 cores, 96 GB of DDR RAM, and 16 GB of MCDRAM. These nodes are connected via a 100 Gb/sec fat-tree Omni-Path interconnect. We use Intel compilers and the MKL library for threaded BLAS routines within Cyclops, including batched BLAS routines, which are efficient for Khatri-Rao products in CP decomposition. We use 8 processes per node and 8 threads per process for all experiments. While this configuration does not use all cores/threads of Stampede2, it generally provided the best or nearly the best performance rate across different node counts. We do not use the sparse tensor functionality in Cyclops, all storage and computation assumes the tensors are dense.

6.1. Microbenchmark Results. We first consider a parallel scaling analysis to compare the simulation time for one ALS sweep of the dimension tree algorithm and the restart step and approximated step of the pairwise perturbation algorithm. The pairwise perturbation restart step include the construction of the pairwise perturbation operators, and is therefore much slower than the approximated (middle) steps. For strong scaling, we consider order $N = 6$ tensors with dimension $s = 50$ and rank $R = 6$ CP and Tucker decompositions. For weak scaling, on p processors, we consider order $N = 6$ tensors with dimension $s = \lfloor 32p^{1/6} \rfloor$ and rank $R = \lfloor 4p^{1/6} \rfloor$.

For weak scaling, Figure 2 shows that with the increase of number of nodes, the step time for all three steps increases. The middle step time of pairwise perturbation is always much faster (7.8 and 10.5 times faster on 1 node and 256 nodes, respectively, compared to the dimension tree based ALS step time) than the other two steps, showing the good scalability of pairwise perturbation. For strong scaling, the figure shows that the middle step time of pairwise perturbation increases with the number of nodes, while the other two step times decrease. The middle PP step is much cheaper computationally and become dominated by communication with increasing node counts, thereby slowing down in step time. For the other two steps, the matrix calculation time will be decreased a lot with the increase of node number, thereby the step time is decreased. Overall, we observe that the potential performance benefit of pairwise perturbation is greater for weak scaling.

6.2. Synthetic Tensor Results. We use three synthetic tensors datasets to test the performance of pairwise perturbation:

- 1. Tensors with random collinearity and noise [7].** We create tensors based on known randomly-generated weight vectors λ and factor matrices $\mathbf{A}^{(n)}$. The weight

¹Our implementations are v1.0.0 of <https://github.com/LinjianMa/pairwise-perturbation>.

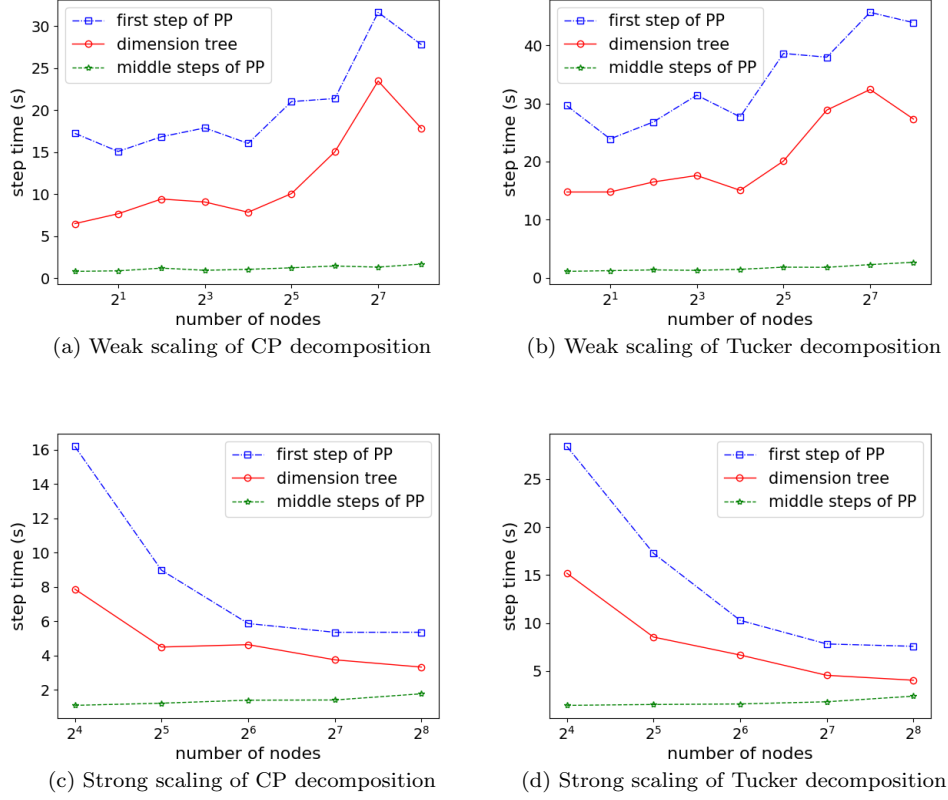


FIGURE 2. Benchmark results for ALS sweeps, taken as the mean time across 5 iterations.

vector $\lambda \in \mathbb{R}^R$ has entries drawn uniformly from $[0.2, 0.8]$, where R is the true rank of the tensor. The factor matrices $\mathbf{A}(n) \in \mathbb{R}^{s \times R}$ are randomly generated so that the columns have collinearity defined by matrix $\mathbf{C} \in [0.5, 0.9]^{R \times R}$, so that,

$$\mathbf{C}(i, j) = \frac{\langle \mathbf{a}_i^{(n)}, \mathbf{a}_j^{(n)} \rangle}{\|\mathbf{a}_i^{(n)}\|_2 \|\mathbf{a}_j^{(n)}\|_2}.$$

Higher collinearity corresponds to greater overlap between factors, which makes the original factors harder to recover using CP-ALS [42]. Additionally, we add noise to the tensor. Let $\mathcal{N} \in \mathbb{R}^{\otimes_{i=1}^N s}$ be a tensor with entries drawn from a uniform random distribution. The tensor we aim to decompose is

$$\boldsymbol{\chi} = \boldsymbol{\chi}_{true} + \eta \left(\frac{\|\boldsymbol{\chi}_{true}\|_2}{\|\mathcal{N}\|_2} \right) \mathcal{N} \quad \text{with} \quad \boldsymbol{\chi}_{true} = \sum_{r=1}^R \lambda_r \mathbf{a}_r^{(1)} \circ \dots \circ \mathbf{a}_r^{(N)},$$

where η controls the magnitude of noise. In the experiments, we set η to 0.01.

2. **Compact Laplacian tensors.** We transpose and unfold the Laplacian tensor so

$$\boldsymbol{\chi} = \sum_{k=1}^d \underbrace{\text{vec}(\mathbf{I}) \circ \dots \circ \text{vec}(\mathbf{I})}_{k-1} \circ \text{vec}(\mathbf{D}) \circ \underbrace{\text{vec}(\mathbf{I}) \circ \dots \circ \text{vec}(\mathbf{I})}_{d-k}.$$

Consequently, \mathcal{X} is an order d equidimensional tensor with CP rank d . We will approximate them with rank 2 CP decomposition.

3. **Tensors made by random matrices.** We create tensors based on known uniformly distributed randomly-generated factor matrices $\mathbf{A}^{(n)} \in [0, 1]^{s \times R}$,

$$\mathcal{X} = \llbracket \mathbf{A}^{(1)}, \dots, \mathbf{A}^{(N)} \rrbracket,$$

In the experiments, we set R to be the same as the decomposition rank.

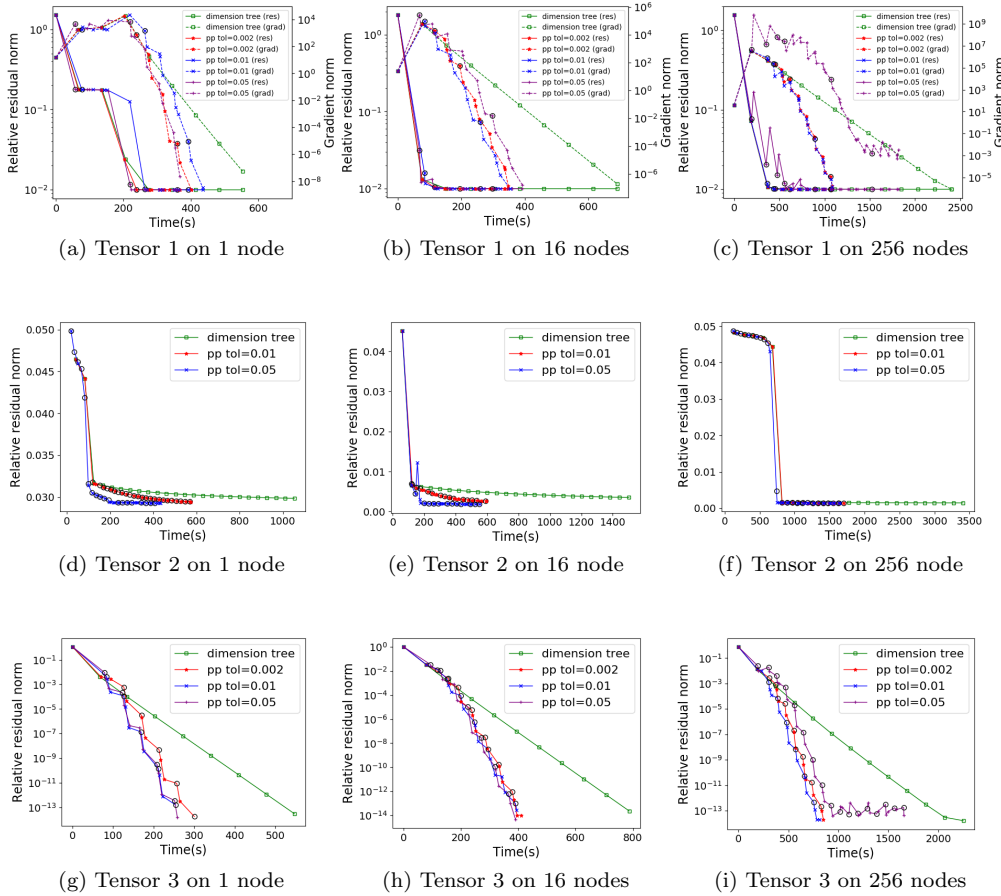


FIGURE 3. Simulation time and relative residual norm comparisons between pairwise perturbation with different tolerance and dimension tree algorithm for CP decomposition. Squares on the dimension tree line represent the results per 10 ALS iterations, and the black circles on pairwise perturbation lines represent the time when pairwise perturbation restarts.

We tested the synthetic tensors for CP decomposition. These tensors all have low ranks and are suitable for testing the speed-up from pairwise perturbation. For tensor 1 and tensor 3, on p processors, we consider order $N = 6$ tensors with dimension $s = \lfloor 32p^{1/6} \rfloor$ and rank $R = \lfloor 4p^{1/6} \rfloor$. For tensor 2, on p processors, we consider order $N = 4$ tensors with dimension $s = \lfloor 169p^{1/4} \rfloor$ and rank $R = 2$.

We display the relative residual norm and execution time for each CP decomposition problem in Figure 3. We observe that pairwise perturbation achieves a lower

execution time for all tensors. For Figure 3a, 3b and 3c, due to the rapid decrease of the residual in the initial steps, we also plot the gradient norm, which controls convergence. Pairwise perturbation performs best for larger tensor sizes, which is consistent with our cost analysis. The speedup for Tensor 1 is 1.5-2.2X, for Tensor 2 is 1.8-2.7X, and for Tensor 3 is 2.0-2.8X. Additionally, different PP restarting tolerance (0.002, 0.01 and 0.05) are shown, which restart the pairwise perturbation scheme when the relative norm difference of each decomposed matrix between two neighboring steps exceeds the tolerance. We can see that for small tensors (shown in Figure 3a, 3d and 3g), a loose tolerance (0.05) can start the pairwise perturbation earlier, leading to relatively better performance. However, when the tensor size is large (shown in Figure 3c and 3i), this loose tolerance (0.05) may lead to the instability of the convergence procedure.

We also note that pairwise perturbation often achieves a lower final residual (most noticeably in Figure 3e). For Figure 3e, the residual norm with tolerance 0.01, 0.05 is 0.53, 0.74 times the residual norm of normal ALS, respectively. This phenomena may be due to the introduction of noise by the perturbative approximation, allowing ALS to find a smaller local minima (similar observations have been made by approximate randomized ALS schemes [7]).

6.3. Tensor Application Dataset Results. We use two application datasets to test the performance benefits of pairwise perturbation:

1. **COIL Data Set.** COIL-100 is an image-recognition data set that contains images of objects in different poses [36] and has been used previously as a tensor decomposition benchmark [7, 50]. There are 100 different object classes, each of which is imaged from 72 different angles. Each image has 128×128 pixels in three color channels. Transferring the data into tensor format, we have a $128 \times 128 \times 3 \times 7200$ tensor. We fix the CP decomposition rank to be 10 and the Tucker decomposition rank to be $10 \times 10 \times 3 \times 70$.
2. **Time-Lapse Hyperspectral Radiance Images.** We consider the 3D hyperspectral imaging dataset called “Souto wood pile” [35]. The dataset is usually used on the benchmark of nonnegative tensor decomposition [5, 31]. The hyperspectral data consists of a tensor with dimensions $1024 \times 1344 \times 33 \times 9$. We fix the CP decomposition rank to be 10 and the Tucker decomposition rank to be $100 \times 100 \times 10 \times 5$.

We display the relative residual norm and execution time for CP decomposition of the two real datasets in Figure 4a, 4b. We observe that pairwise perturbation achieves a lower execution time for them. The speedup for the Coil Dataset is 1.5-2.0X and for the Time-Lapse Dataset is 2.1-2.5X. Additionally, a larger PP restarting tolerance (0.1) leads to better performance.

Pairwise perturbation is also used to speedup HOOI procedure in Tucker decomposition. However, as noted in other work [4], we observed that ALS iterations do not significantly lower the residual beyond what is achieved by the first iteration (HOSVD). Nevertheless, we study the benefit of pairwise perturbation on reaching convergence of ALS faster (it is possible that a more practical benefit from pairwise perturbation would be achieved for variations of Tucker decomposition that enforce additional constraints or for other tensors).

We display the relative residual norm, the relative norm change of core tensor and execution time for Tucker decomposition of the two real datasets in Figure 4c, 4d. The speedup for the Coil Dataset is 1.02-1.04X and for the Time-Lapse Dataset is 1.11-1.28X. The reason for no obvious speed-up for the Coil Dataset is that the tensor

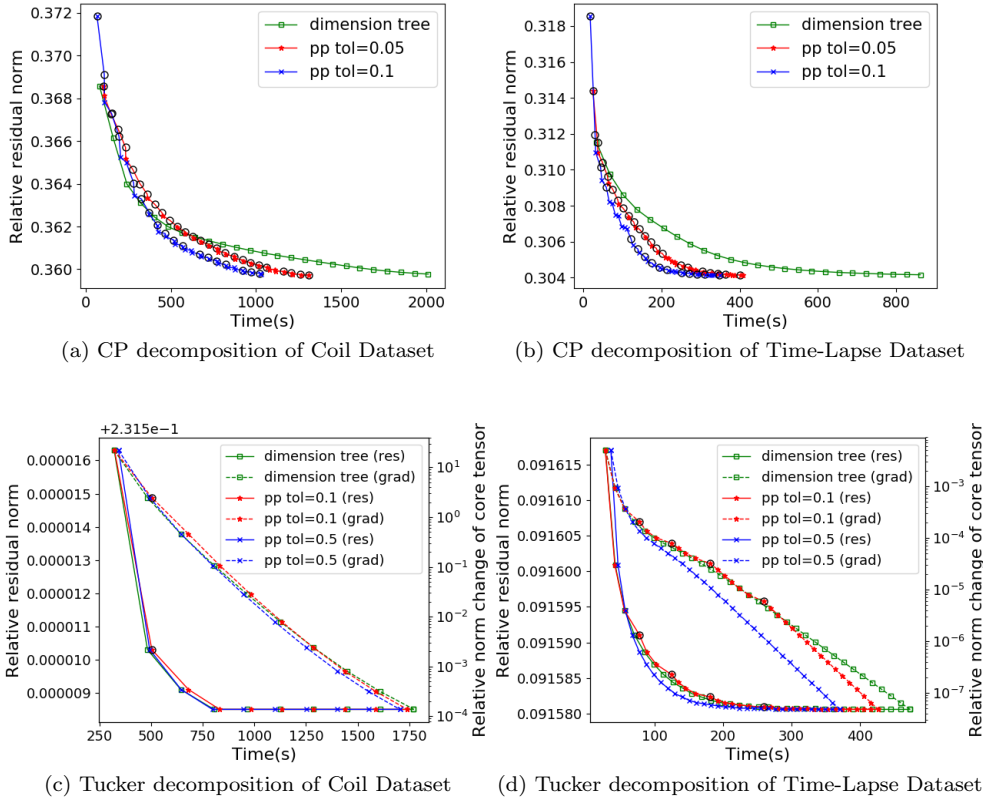


FIGURE 4. *Experimental results between pairwise perturbation and dimension tree algorithm for CP and tucker decompositions on 1 KNL node. Each dot on the dimension tree/PP lines represents the results per 10 ALS iterations for CP and per ALS iteration for Tucker decomposition, and the black circles on pairwise perturbation lines represent the time when pairwise perturbation restarts.*

is not equidimensional (one dimension is 7200, while others are all smaller or equal to 128). Therefore, when updating the factor matrix with a dimension of 7200, the number of operations necessary to construct the SVD input for PP are similar to that for the dimension tree Tucker algorithm. For the Time-Lapse Dataset, the tensor dimensions are more evenly distributed (two dimensions are greater than 1000), and we observe a greater speed-up. We conclude that the proposed Tucker PP algorithm performs better when used on the tensors whose dimensions are approximately equal.

7. Conclusion. We have provided a pairwise perturbation algorithm for both CP and Tucker decompositions for dense tensors. The advantage of this algorithm is that it uses perturbative corrections rather than recomputing the tensor contractions to set up the quadratic optimization subproblems, and is accurate when the factor matrices change little, based on our error analysis. Specifically, our Cyclops implementation of pairwise perturbation shows speed-ups for CP-ALS of 1.5-2.8X across all synthetic and application data with respect to the best known method for exact CP-ALS (also implemented with Cyclops).

We leave analysis and benchmarking of pairwise perturbation with sparse tensors

for future work. Since contraction between the input tensor and the first factor matrix will require fewer operations, the benefit of pairwise perturbation is likely to be lesser. Additionally, it is likely of interest to investigate more efficient adaptations of pairwise perturbation for non-equidimensional tensors and to experiment with alternative schemes for switching between regular ALS and pairwise perturbation.

The new notion of tensor condition number (Section 3.2), which we used in the error bounds derived in Section 5 also leaves many directions for future work. It is unclear how to construct tensors of arbitrary order and dimension with bounded condition number or how to efficiently bound the condition number for a given tensor.

REFERENCES

- [1] E. Acar, D. M. Dunlavy, and T. G. Kolda. A scalable optimization approach for fitting canonical tensor decompositions. *Journal of Chemometrics*, 25(2):67–86, 2011.
- [2] A. Anandkumar, R. Ge, D. J. Hsu, S. M. Kakade, and M. Telgarsky. Tensor decompositions for learning latent variable models. *Journal of Machine Learning Research*, 15(1):2773–2832, 2014.
- [3] C. A. Andersson and R. Bro. Improving the speed of multi-way algorithms: Part I. Tucker3. *Chemometrics and intelligent laboratory systems*, 42(1-2):93–103, 1998.
- [4] W. Austin, G. Ballard, and T. G. Kolda. Parallel tensor compression for large-scale scientific data. In *Parallel and Distributed Processing Symposium, 2016 IEEE International*, pages 912–922. IEEE, 2016.
- [5] G. Ballard, K. Hayashi, and R. Kannan. Parallel nonnegative CP decomposition of dense tensors. *arXiv preprint arXiv:1806.07985*, 2018.
- [6] G. Ballard, N. Knight, and K. Rouse. Communication lower bounds for matricized tensor times Khatri-Rao product. In *2018 IEEE International Parallel and Distributed Processing Symposium (IPDPS)*, pages 557–567. IEEE, 2018.
- [7] C. Battaglino, G. Ballard, and T. G. Kolda. A practical randomized CP tensor decomposition. *SIAM Journal on Matrix Analysis and Applications*, 39(2):876–901, 2018.
- [8] U. Benedikt, H. Auer, M. Espig, W. Hackbusch, and A. A. Auer. Tensor representation techniques in post-Hartree–Fock methods: matrix product state tensor format. *Molecular Physics*, 111(16-17):2398–2413, 2013.
- [9] L. S. Blackford, J. Choi, A. Cleary, E. D’Azevedo, J. Demmel, I. Dhillon, S. Hammarling, G. Henry, A. Petitet, K. Stanley, D. Walker, and R. C. Whaley. *ScaLAPACK User’s Guide*. Society for Industrial and Applied Mathematics, Philadelphia, PA, USA, 1997.
- [10] P. Breiding and N. Vannieuwenhoven. The condition number of join decompositions. *SIAM Journal on Matrix Analysis and Applications*, 39(1):287–309, 2018.
- [11] J. D. Carroll and J.-J. Chang. Analysis of individual differences in multidimensional scaling via an n-way generalization of Eckart-Young decomposition. *Psychometrika*, 35(3):283–319, 1970.
- [12] V. T. Chakaravarthy, J. W. Choi, D. J. Joseph, X. Liu, P. Murali, Y. Sabharwal, and D. Sreedhar. On optimizing distributed Tucker decomposition for dense tensors. In *Parallel and Distributed Processing Symposium (IPDPS), 2017 IEEE International*, pages 1038–1047. IEEE, 2017.
- [13] J. Choi, X. Liu, and V. Chakaravarthy. High-performance dense Tucker decomposition on GPU clusters. In *Proceedings of the International Conference for High Performance Computing, Networking, Storage, and Analysis*, page 42. IEEE Press, 2018.
- [14] A. Cichocki, N. Lee, I. Oseledets, A.-H. Phan, Q. Zhao, and D. P. Mandic. Tensor networks for dimensionality reduction and large-scale optimization: Part 1 low-rank tensor decompositions. *Foundations and Trends in Machine Learning*, 9(4-5):249–429, 2016.
- [15] L. De Lathauwer, B. De Moor, and J. Vandewalle. A multilinear singular value decomposition. *SIAM journal on Matrix Analysis and Applications*, 21(4):1253–1278, 2000.
- [16] L. De Lathauwer, B. De Moor, and J. Vandewalle. On the best rank-1 and rank-(r_1, r_2, \dots, r_n) approximation of higher-order tensors. *SIAM journal on Matrix Analysis and Applications*, 21(4):1324–1342, 2000.
- [17] V. De Silva and L.-H. Lim. Tensor rank and the ill-posedness of the best low-rank approximation problem. *SIAM Journal on Matrix Analysis and Applications*, 30(3):1084–1127, 2008.
- [18] L. Grasedyck, D. Kressner, and C. Tobler. A literature survey of low-rank tensor approximation techniques. *GAMM-Mitteilungen*, 36(1):53–78, 2013.

- [19] W. Hackbusch. Tensor spaces and numerical tensor calculus, volume 42. Springer Science & Business Media, 2012.
- [20] N. Hao, L. Horesh, and M. Kilmer. Nonnegative tensor decomposition. In Compressed Sensing & Sparse Filtering, pages 123–148. Springer, 2014.
- [21] R. A. Harshman. Foundations of the PARAFAC procedure: models and conditions for an explanatory multimodal factor analysis. 1970.
- [22] K. Hayashi, G. Ballard, J. Jiang, and M. Tobia. Shared memory parallelization of MTTKRP for dense tensors. arXiv preprint arXiv:1708.08976, 2017.
- [23] F. L. Hitchcock. The expression of a tensor or a polyadic as a sum of products. Studies in Applied Mathematics, 6(1-4):164–189, 1927.
- [24] E. G. Hohenstein, R. M. Parrish, and T. J. Martínez. Tensor hypercontraction density fitting. I. Quartic scaling second- and third-order Møller-Plesset perturbation theory. The Journal of Chemical Physics, 137(4):044103, 2012.
- [25] T. Huckle, K. Waldherr, and T. Schulte-Herbrüggen. Computations in quantum tensor networks. Linear Algebra and its Applications, 438(2):750 – 781, 2013. Tensors and Multilinear Algebra.
- [26] F. Hummel, T. Tsatsoulis, and A. Grüneis. Low rank factorization of the coulomb integrals for periodic coupled cluster theory. The Journal of chemical physics, 146(12):124105, 2017.
- [27] L. Karlsson, D. Kressner, and A. Uschmajew. Parallel algorithms for tensor completion in the CP format. Parallel Computing, 57:222–234, 2016.
- [28] O. Kaya and B. Uçar. High performance parallel algorithms for the Tucker decomposition of sparse tensors. In Parallel Processing (ICPP), 2016 45th International Conference on, pages 103–112. IEEE, 2016.
- [29] O. Kaya and B. Uçar. Parallel CP decomposition of sparse tensors using dimension trees. PhD thesis, Inria-Research Centre Grenoble–Rhône-Alpes, 2016.
- [30] T. G. Kolda and B. W. Bader. Tensor decompositions and applications. SIAM review, 51(3):455–500, 2009.
- [31] A. P. Liavas, G. Kostoulas, G. Lourakis, K. Huang, and N. D. Sidiropoulos. Nesterov-based alternating optimization for nonnegative tensor factorization: Algorithm and parallel implementation. IEEE Trans. Signal Process, 66:944–953, 2017.
- [32] L.-H. Lim. Singular values and eigenvalues of tensors: a variational approach. In Computational Advances in Multi-Sensor Adaptive Processing, 2005 1st IEEE International Workshop on, pages 129–132. IEEE, 2005.
- [33] J. Liu, P. Musialski, P. Wonka, and J. Ye. Tensor completion for estimating missing values in visual data. IEEE Transactions on Pattern Analysis and Machine Intelligence, 35(1):208–220, 2013.
- [34] J. G. Nagy and M. E. Kilmer. Kronecker product approximation for preconditioning in three-dimensional imaging applications. IEEE Transactions on Image Processing, 15(3):604–613, March 2006.
- [35] S. M. Nascimento, K. Amano, and D. H. Foster. Spatial distributions of local illumination color in natural scenes. Vision Research, 120:39–44, 2016.
- [36] S. A. Nene, S. K. Nayar, and H. Murase. Columbia object image library (coil-100).
- [37] R. Orús. A practical introduction to tensor networks: Matrix product states and projected entangled pair states. Annals of Physics, 349:117 – 158, 2014.
- [38] I. V. Oseledets and E. E. Tyrtysnikov. Breaking the curse of dimensionality, or how to use SVD in many dimensions. SIAM Journal on Scientific Computing, 31(5):3744–3759, 2009.
- [39] W. Pazner and P.-O. Persson. Approximate tensor-product preconditioners for very high order discontinuous galerkin methods. Journal of Computational Physics, 354:344–369, 2018.
- [40] I. Perros, R. Chen, R. Vuduc, and J. Sun. Sparse hierarchical Tucker factorization and its application to healthcare. In Data Mining (ICDM), 2015 IEEE International Conference on, pages 943–948. IEEE, 2015.
- [41] A.-H. Phan, P. Tichavský, and A. Cichocki. Fast alternating LS algorithms for high order CANDECAMP/PARAFAC tensor factorizations. IEEE Transactions on Signal Processing, 61(19):4834–4846, 2013.
- [42] M. Rajih, P. Comon, and R. A. Harshman. Enhanced line search: A novel method to accelerate parafac. SIAM journal on matrix analysis and applications, 30(3):1128–1147, 2008.
- [43] M. D. Schatz, T. M. Low, R. A. van de Geijn, and T. G. Kolda. Exploiting symmetry in tensors for high performance: Multiplication with symmetric tensors. SIAM Journal on Scientific Computing, 36(5):C453–C479, 2014.
- [44] E. Solomonik, D. Matthews, J. R. Hammond, J. F. Stanton, and J. Demmel. A massively parallel tensor contraction framework for coupled-cluster computations. Journal of Parallel and Distributed Computing, 74(12):3176–3190, 2014.

- [45] P. Springer, T. Su, and P. Bientinesi. HPTT: a high-performance tensor transposition C++ library. In Proceedings of the 4th ACM SIGPLAN International Workshop on Libraries, Languages, and Compilers for Array Programming, pages 56–62. ACM, 2017.
- [46] L. R. Tucker. Some mathematical notes on three-mode factor analysis. Psychometrika, 31(3):279–311, 1966.
- [47] N. Vannieuwenhoven. Condition numbers for the tensor rank decomposition. Linear Algebra and Its Applications, 535:35–86, 2017.
- [48] N. Vannieuwenhoven, K. Meerbergen, and R. Vandebril. Computing the gradient in optimization algorithms for the CP decomposition in constant memory through tensor blocking. SIAM Journal on Scientific Computing, 37(3):C415–C438, 2015.
- [49] N. Vannieuwenhoven, R. Vandebril, and K. Meerbergen. A new truncation strategy for the higher-order singular value decomposition. SIAM Journal on Scientific Computing, 34(2):A1027–A1052, 2012.
- [50] G. Zhou, A. Cichocki, and S. Xie. Decomposition of big tensors with low multilinear rank. arXiv preprint arXiv:1412.1885, 2014.